

## STEM CELLS AND REGENERATION

## RESEARCH ARTICLE

# Lineage-specific reorganization of nuclear peripheral heterochromatin and H3K9me2 domains

Kelvin See<sup>1,2,3,4</sup>, Yemin Lan<sup>2,4</sup>, Joshua Rhoades<sup>1,2,3,4,5</sup>, Rajan Jain<sup>1,2,3</sup>, Cheryl L. Smith<sup>1,2,3,4</sup> and Jonathan A. Epstein<sup>1,2,3,4,\*</sup>

**ABSTRACT**

Dynamic organization of chromatin within the three-dimensional nuclear space has been postulated to regulate gene expression and cell fate. Here, we define the genome-wide distribution of nuclear peripheral heterochromatin as a multipotent P19 cell adopts either a neural or a cardiac fate. We demonstrate that H3K9me2-marked nuclear peripheral heterochromatin undergoes lineage-specific reorganization during cell-fate determination. This is associated with spatial repositioning of genomic loci away from the nuclear periphery as shown by 3D immuno-FISH. Locus repositioning is not always associated with transcriptional changes, but a subset of genes is upregulated. *Mef2c* is specifically repositioned away from the nuclear periphery during early neurogenic differentiation, but not during early cardiogenic differentiation, with associated transcript upregulation. *MyoCD* is specifically repositioned during early cardiogenic differentiation, but not during early neurogenic differentiation, and is transcriptionally upregulated at later stages of cardiac differentiation. We provide experimental evidence for lineage-specific regulation of nuclear architecture during cell-fate determination in a mouse cell line.

**KEY WORDS:** H3K9me2 domains, Nuclear architecture, Nuclear peripheral heterochromatin

**INTRODUCTION**

A recent focus of research on gene regulation and epigenetics involves understanding the mechanisms by which DNA is packaged within the nucleus, and how this packaging and organization is dynamically regulated over time in specific cell types. This has been the focus of the federally funded ‘4D Nucleome Project’ (Dekker et al., 2017) among many other research programs. One mechanism of chromatin organization involves localization of specific regions of the genome to the nuclear periphery in so-called lamina associated domains (LADs) (Guelen et al., 2008). LADs have been characterized as transcriptionally repressive heterochromatin at the nuclear periphery (Guelen et al., 2008; van Steensel and Belmont, 2017). Recent efforts to identify changes in LADs during differentiation of mouse embryonic stem cells (mESCs) to neural

precursors and astrocytes implicate a reorganization of LADs during neuronal differentiation (Dekker et al., 2017; Guelen et al., 2008; Peric-Hupkes et al., 2010). *Drosophila* neuroblasts undergo developmentally regulated sub-nuclear genome reorganization of the *hunchback* gene locus that correlates with loss of progenitor competence (Guelen et al., 2008; Kohwi et al., 2013). Likewise, differentiation of C2C12 myoblasts into myotubes suggests that there may be repositioning of myogenic genes away from the periphery during myogenic differentiation (Guelen et al., 2008; Robson et al., 2016; van Steensel and Belmont, 2017). Nevertheless, it remains unclear whether lineage-specific spatial reorganization of nuclear peripheral heterochromatin accompanies lineage specification when the multipotent progenitor cell adopts different cell fates in a single system.

We sought to examine lineage-specific chromatin organization and nuclear peripheral heterochromatin changes that occur during the acquisition of different cell fates. Using a reductionist approach, we assessed changes in nuclear peripheral heterochromatin in P19 multipotent embryonal carcinoma cells, which are competent to adopt a neurogenic or a cardiogenic fate in a simple, well-established model system. P19 cells are karyotypically normal cells that are multipotent and able to form cells of all three germ layers when injected into blastocysts (Rossant and McBurney, 1982). They differentiate into neuronal cells upon exposure to retinoic acid (Jones-Villeneuve, 1982) or into cardiomyocytes and skeletal muscle upon exposure to dimethyl sulfoxide (DMSO) (Edwards et al., 1983; Jasmin et al., 2010). Our group and others have recently reported that the histone modification H3K9me2 is specifically associated with LADs and is restricted to nuclear peripheral heterochromatin (Kind et al., 2013; Peric-Hupkes et al., 2010; Poleshko et al., 2017; van Steensel and Belmont, 2017). We used H3K9me2 ChIP-seq to monitor changes in nuclear peripheral heterochromatin in the P19 differentiation system as cells specifically adopted a neuronal fate or cardiac mesodermal fate.

Here, we report that there is dynamic local reorganization of nuclear peripheral heterochromatin during cell-fate acquisition that is specific to the particular cell fate being adopted. In addition, we demonstrate that genomic loci of crucial developmental master regulators are released from the nuclear periphery according to the specific cell fate during this process. This provides evidence that spatial organization of chromatin with respect to the nuclear periphery provides a layer of regulation that is specific to the distinct cell fate acquired.

**RESULTS****P19 cells are competent to adopt neuronal or cardiac cell fates**

Using well established protocols (Jasmin et al., 2010; Martins et al., 2005), multipotent P19 embryonal carcinoma cells can be induced to differentiate along separate cell lineages. To promote

<sup>1</sup>Department of Medicine, Perelman School of Medicine, University of Pennsylvania, PA 19104, USA. <sup>2</sup>Department of Cell and Developmental Biology, Perelman School of Medicine, University of Pennsylvania, PA 19104, USA. <sup>3</sup>Institute for Regenerative Medicine, Penn Cardiovascular Institute, Perelman School of Medicine, University of Pennsylvania, PA 19104, USA. <sup>4</sup>Penn Epigenetics Institute, Perelman School of Medicine, University of Pennsylvania, PA 19104, USA. <sup>5</sup>Institute for Biomedical Informatics, Perelman School of Medicine, University of Pennsylvania, PA 19104, USA.

\*Author for correspondence (epsteinj@pennmedicine.upenn.edu)

✉ K.S., 0000-0003-0647-6977; J.A.E., 0000-0001-8637-4465

Received 22 November 2018; Accepted 8 January 2019

differentiation along a neuronal lineage, P19 cells were cultured with 1 µM *all-trans* retinoic acid (RA). Alternately, to differentiate cells along a mesodermal lineage, cells were grown in 1% DMSO (Fig. 1A). Undifferentiated P19 cells were cultured at low density to prevent ectopic differentiation and to maintain multipotency. The morphologies of RA-treated and DMSO-treated cells were distinct at later stages of treatment: RA-treated cells displayed long cellular processes that resembled neurite extensions by day 5 (Fig. S1), whereas spontaneous beating foci were observed in DMSO-treated

cultures by day 10 (Movie 1). In addition to monitoring morphology, we compared protein levels of several known markers of differentiation 3 days after each treatment and in the undifferentiated cells. The pluripotency marker Oct4 (also known as Pou5f1) was downregulated at day 3 (D3) in both RA- and DMSO-treated cells, which indicates loss of pluripotency by D3 in both treatment conditions (Fig. 1B). RA treatment resulted in specific upregulation of the neurogenic transcription factor EphA3 at D3 (Fig. 1B). DMSO treatment induced specific upregulation of the

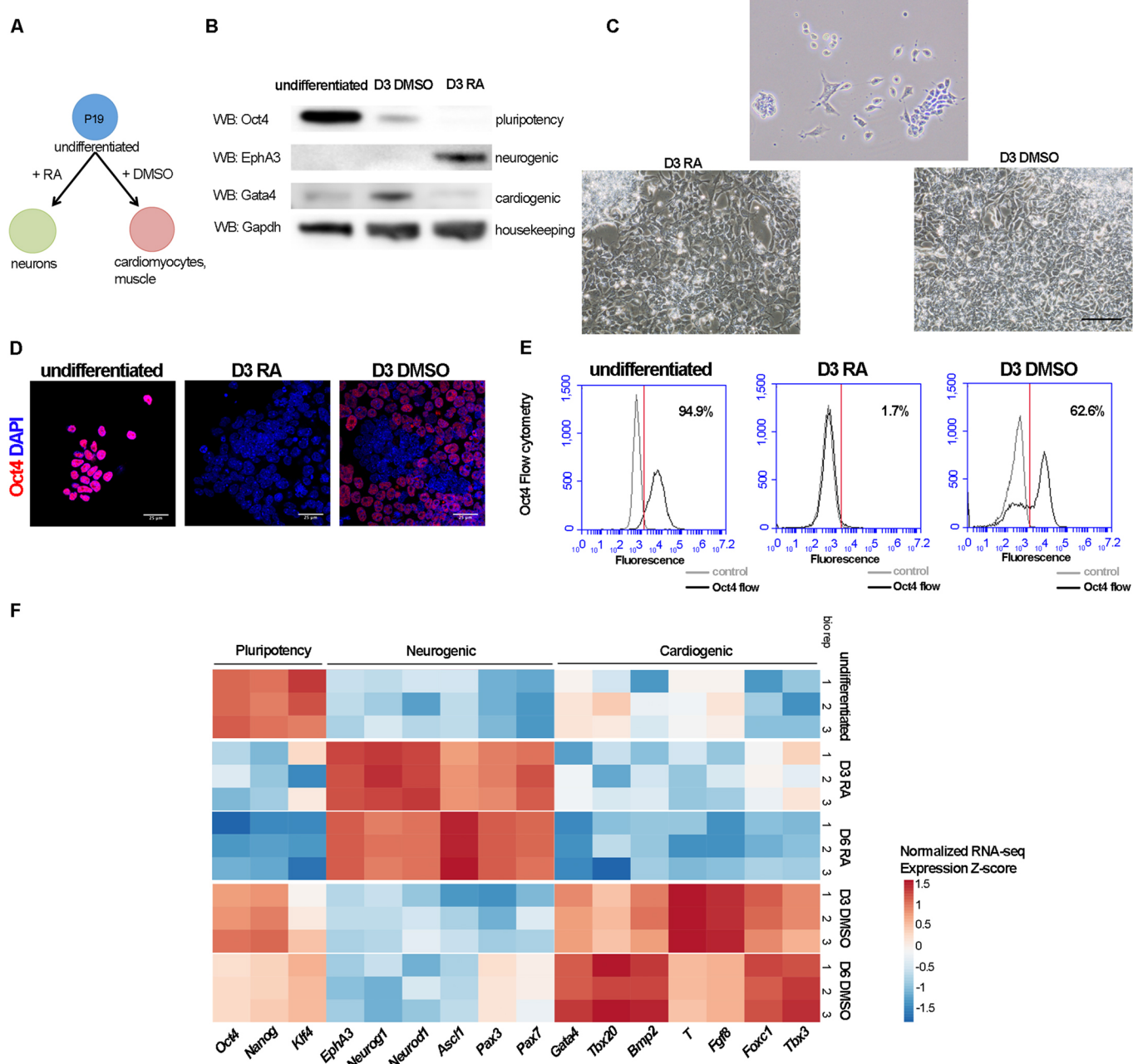


**Fig. 1. P19 cells are competent to adopt a neural fate or cardiac fate in a model system of cell-fate choice.** (A) Scheme for differentiation of P19 cells. (B) Western Blot (WB) of pluripotency marker (Oct4), neurogenic transcription factor (EphA3), cardiogenic transcription factor (Gata4) and housekeeping marker (Gapdh) during differentiation of P19 cells. (C) Representative images of undifferentiated P19, D3 RA- and D3 DMSO-treated cells. (D) Immunofluorescence of pluripotency factor Oct4 in undifferentiated, D3 RA- and D3 DMSO-treated P19 cells. (E) Flow cytometry of undifferentiated, D3 RA- and D3 DMSO-treated P19 cells stained for Oct4 to determine the percentage of Oct4<sup>+</sup> cells. Gray line represents negative control; black line represents Oct4-stained sample. (F) Heatmap representation of RNA-seq of P19 cells during differentiation. bio rep, biological replicate. Normalized RNA-seq expression z-score provided. Scale bars: 250 µm in C; 25 µm in D.

cardiogenic transcription factor *Gata4* at D3 (Fig. 1B). This suggests that the molecular markers of cell-fate specification were expressed at D3, even before the observed morphological changes that were induced by DMSO or RA (Fig. 1C).

Using both immunofluorescence and flow cytometry, we found that pluripotency factor Oct4 was highly expressed in almost all undifferentiated cells (94.9% by flow cytometry; Fig. 1D,E) but was found to be dramatically depleted to ~1.7% Oct4<sup>+</sup> cells after 3 days of RA treatment, and reduced to ~62.6% Oct4<sup>+</sup> cells after 3 days of DMSO treatment (Fig. 1D,E). This suggests that D3 RA-treated cells were more efficiently differentiated compared with D3 DMSO-treated cells.

To further characterize the differences between RA- and DMSO-treated P19 cells, we assessed global changes in gene expression at early stages of differentiation, before morphological changes were readily apparent. We extracted RNA and performed RNA-seq on three biological replicates each of undifferentiated P19 cells as well as RA- and DMSO-differentiated cells that had been treated for 3 days or 6 days. Relative levels of gene expression for replicates of each condition cluster together, and the overall pattern of changes in transcription reveals clear differences between D3 RA- and D3 DMSO-treated cells (Fig. 1F). Differential gene expression reflects a transition from undifferentiated towards either a neurogenic fate following 3 days of RA treatment (upregulation of genes involved in nervous system development, axon guidance and neurogenesis; Table S1, Fig. S2A) or a cardiac mesodermal fate after 3 days of DMSO treatment (upregulation of genes required for somitogenesis, heart morphogenesis and heart development; Table S2, Fig. S2B). Following differentiation in either condition, a number of genes that encode pluripotency factors (*Oct4*, *Nanog*, *Klf4*) were downregulated (Fig. 1F).

The D3 and day 6 (D6) RNA-seq data demonstrate that specific differences in transcript abundance discriminate between treatment conditions. Several neurogenic transcription factors, including *EphA3*, *Neurog1*, *Neurod1*, *Ascl1*, *Pax3* and *Pax7* were specifically upregulated in D3 RA-treated cells, but not in D3 DMSO-treated cells (Fig. 1F). Cardiogenic transcription factors, including *Gata4*, *Tbx20*, *Bmp2*, *T*, *Fgf8*, *Foxc1* and *Tbx3* were specifically upregulated in D3 DMSO-treated cells, but not in D3 RA-treated cells (Fig. 1F). We validated a subset of genes by real-time quantitative PCR (RT-qPCR) and confirmed the depletion of *Oct4* in D3 RA-treated cells and downregulation of *Oct4* in D3 DMSO-treated cells (Fig. S2C), specific upregulation of neurogenic transcription factors (*Pax3*, *Neurog1*) in D3 RA-treated cells (Fig. S2D,E) and specific upregulation of cardiogenic *Gata4* transcription factor in D3 DMSO-treated cells (Fig. S2F). These data demonstrate that P19 cells can be induced to adopt a treatment-specific cell fate – either neuronal or cardiac mesodermal – and that the differences are reflected in distinctive morphologies and gene expression patterns.

### H3K9me2-marked heterochromatin reflects nuclear architecture in P19 cells

To identify the changes in nuclear architecture that accompany lineage specification, we examined the distribution pattern of genome-wide H3K9me2-marked chromatin in undifferentiated P19 cells, and in D3 RA- and D3 DMSO-treated P19 cells. As shown previously, H3K9me2 preferentially marks chromatin at the nuclear periphery and H3K9me2 domains are highly correlated with LADs (Poleshko et al., 2017). We performed H3K9me2 ChIP-seq of undifferentiated D3 RA- and D3 DMSO-treated P19 cells with three biological replicates per condition (Fig. 2A,B; merged biological

replicates for visualization). We chose this time point to assess H3K9me2 domains as molecular markers of lineage specificity were already observed following 3 days of either treatment (Fig. 1F, Tables S1 and S2). Control H3 ChIP-seq was performed in parallel for all samples in order to assess the specific contribution of H3K9me2. The H3K9me2 signal, as assayed in 10 kb bins, was highly correlated within each set of biological replicates [average H3K9me2 ChIP-seq inter-replicate correlation (see Materials and Methods): Spearman's correlation coefficient  $r=0.87$  undifferentiated,  $r=0.94$  RA,  $r=0.9$  DMSO] (Fig. S3A). In comparison, the correlation coefficients across treatment conditions were lower (average of 10 kb bins individual replicates: undifferentiated versus RA,  $r=0.73$ ; undifferentiated versus DMSO,  $r=0.85$ ; RA versus DMSO,  $r=0.84$ ; Fig. S3A). This confirms that there was greater variability across differentiation conditions than within individual biological replicates per condition.

We observed genome-wide coverage of H3K9me2-marked regions in P19 cells to be ~40% of the mouse genome (ranging from 38.5% in undifferentiated to 41.7% in D3 RA and 40.8% in D3 DMSO; Fig. S3B). This is consistent with the genome coverage that is reported for LADs in human fibroblast cells (40%) (Guelen et al., 2008) and various mouse cells (35–43%) (Meuleman et al., 2013; Peric-Hupkes et al., 2010; Poleshko et al., 2017). The H3K9me2 domains that are found in undifferentiated P19 cells were also similar to the LaminB or H3K9me2 domains that were previously observed in mESCs (Poleshko et al., 2017) (Fig. S3C,D).

### H3K9me2 domains vary according to cell fate

Using Enriched Domain Detector (EDD; Lund et al., 2014), we defined H3K9me2 domains and asked whether these domains varied by treatment in the P19 differentiation system. We performed principal component analysis (PCA) on the genome-wide H3K9me2 domains and leveraged the replicate data to compare domains across differentiation conditions. We found that the three biological replicates were similar and cluster together within each condition, whereas significant variation separates the samples by treatment condition (Fig. 2C, 95% confidence interval ellipses). The H3K9me2 domains were sufficient to accurately distinguish between undifferentiated, D3 RA-treated and D3 DMSO-treated P19 cells.

To assess the extent of similarity across the various conditions, we also measured the Jaccard indices and found that the H3K9me2 domains in undifferentiated samples showed differences between either D3 RA- or D3 DMSO-treated samples (undifferentiated versus D3 RA=0.76, undifferentiated versus D3 DMSO=0.78; Fig. 2D).

Although a large subset of H3K9me2 domains (68.1% of H3K9me2 domain genome coverage in base pairs) was constitutive across all conditions, there were distinct regions that varied between undifferentiated and differentiated P19 cells (31.9%) (Fig. 2A,B,E). These variable regions include a subset (3.0%) that are found in undifferentiated cells, but absent in both D3 RA- and D3 DMSO-treated samples (shared loss; Fig. 2E). Similarly, 8.3% of H3K9me2-marked domains were not observed in undifferentiated cells, but were present in both RA- and DMSO-treated cells (shared gain; Fig. 2E). Notably, there were twice as many regions (20.6%) that were specific to either the neuronal or myogenic lineage within the set of H3K9me2 domains that changed as a result of differentiation (specific; Fig. 2E). In particular, regions that lost H3K9me2 specifically in RA or DMSO (9.8%) had three times more genome coverage than regions that were lost in both conditions (3.0%) (specific loss versus shared loss; Fig. 2E). There were also

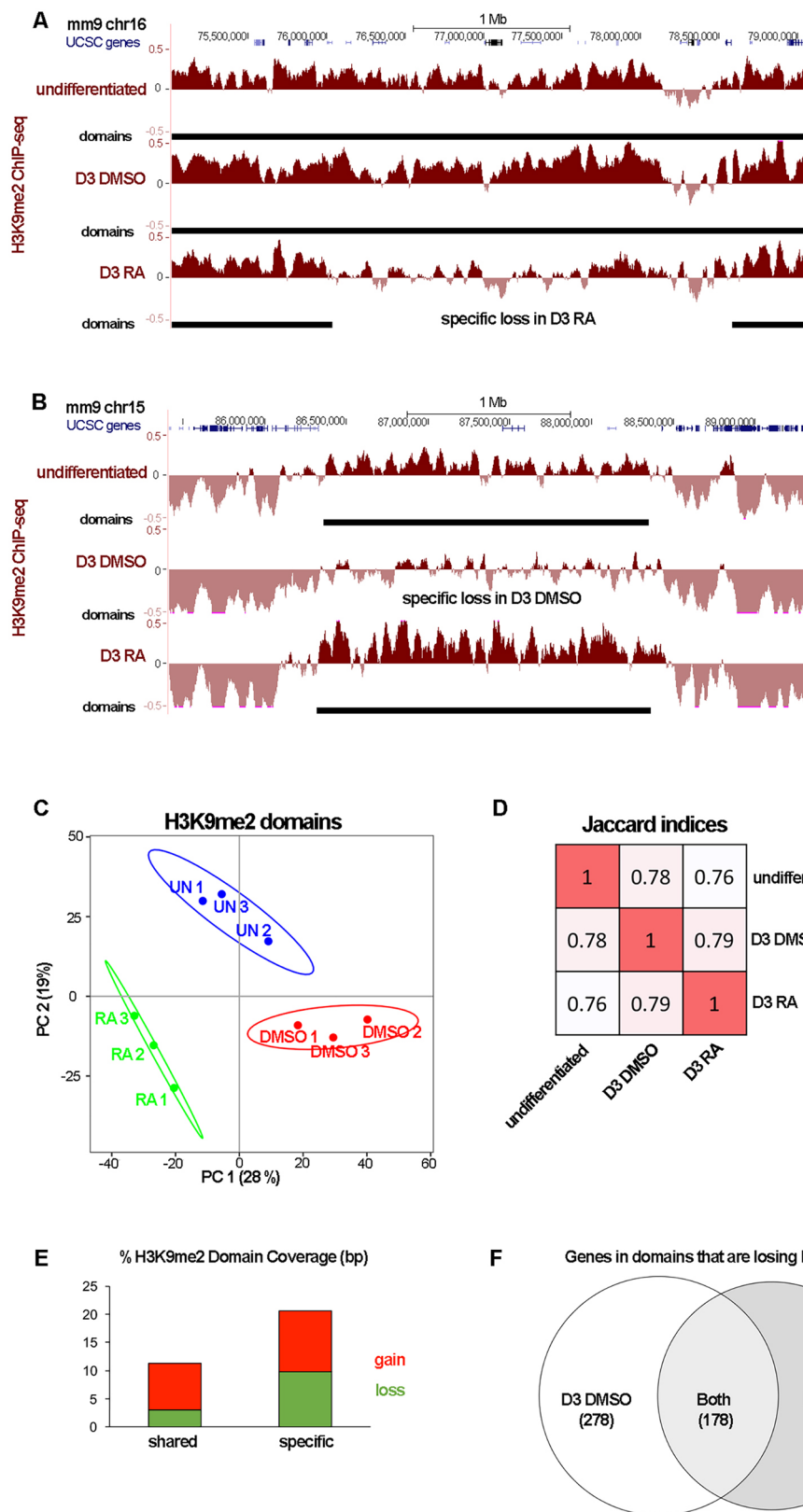


**Fig. 2. H3K9me2-marked nuclear peripheral heterochromatin displays lineage-specific local reorganization during cell-fate choice.** (A,B) Representative merged H3K9me2 ChIP-seq tracks that show regions of specific loss in D3 RA- or in D3 DMSO-treated cells. Black bars indicate H3K9me2 domains called by EDD. (C) PCA plot of H3K9me2 domains accurately stratifies individual biological replicates by treatment condition. Ellipses show 95% confidence interval. UN, undifferentiated; DMSO, D3 DMSO-treated; RA, D3 RA-treated. (D) Jaccard indices of H3K9me2 domains found in undifferentiated, D3 DMSO- or D3 RA-treated P19 cells. (E) Comparison of % H3K9me2 domain coverage (base pairs) in shared or specific regions (D3 DMSO only or D3 RA only). Gain, regions that gained residency within H3K9me2 domains; loss, regions that lost residency within H3K9me2 domains. (F) Number of genes found in H3K9me2 domains that were specifically lost in either D3 DMSO or D3 RA.

more genes found in regions of specific loss in D3 RA-treated or D3 DMSO-treated compared with regions of shared loss (Fig. 2F; Tables S5-S7).

We defined genes to be within the H3K9me2 domains if the gene has at least 75% overlap with H3K9me2 domain (see Materials and

Methods). We then asked whether genes found within regions that lost the identifying H3K9me2 mark during lineage specification had any function relevant to the cell fate the P19 cells would adopt. We found that there were many neuronal genes (*Mef2c*, *Sv2b*, *Nrp1*, *Sox3*, *Dpysl3*, *App*, *Mecom*, *Top2b*, *Ptn*, *Rarb*, *Camk4*, *Gap43*,

*Rai2, St7, Syt10, Tcf4*) with functions that are important for neuronal development that lost the H3K9me2 mark specifically in D3 RA-treated samples (Table S5), which suggests that the genes were highly relevant and specific to the neuronal cell fate being adopted. Conversely, we found that there were many cardiac genes [*Myocd, Gfra2, Ghr, Map2k4, Wisp1 (Ccn4), Nr3c1, Plxna4, Adcy2, Odz2 (Tenn2), Bzw2, Tnik, Pld1, Ptger3, Ndrg1, Prune2, Esrsg, Lmcd1, Lmo7, Palmd, Hmgxb4, Tbc1d4, Sox11, Syne1, Dock1, Zfp161 (Zbtb14), Adamts1*]<sup>1</sup>] that are important for cardiac muscle development that lost the H3K9me2 mark specifically in D3 DMSO-treated samples (Table S6). Importantly, these neuronal or cardiac genes were found in regions that lost the H3K9me2 mark in a lineage-specific fashion. This suggests that genes losing lineage-specific H3K9me2-marked domains and nuclear peripheral localization upon differentiation have functions that are important and specific to the cell fate to be adopted.

#### Genomic loci reposition from the nuclear periphery with lineage specificity

To investigate global cellular changes of the H3K9me2-marked nuclear peripheral heterochromatin during P19 differentiation, we examined H3K9me2 by immunofluorescence in undifferentiated, D3 RA-treated and D3 DMSO-treated cells. Using high-resolution confocal microscopy to visualize H3K9me2, we observed H3K9me2-marked heterochromatin at the nuclear periphery, adjacent to the nuclear lamina, in both undifferentiated and differentiated P19 cells (Fig. 3A). There was no apparent alteration in the nuclear peripheral heterochromatin layer as assessed by the thickness of the H3K9me2 immunofluorescent signal following DMSO or RA treatment compared with untreated cells (average thickness 0.34 µm; Fig. 3B). We also examined the total amount of the H3K9me2 modification in nuclear lysates by western blot (Fig. 3C). We observed very similar levels of H3K9me2 (normalized to total H3) in nuclear lysates from untreated and differentiated P19 cells (Fig. 3D).

We hypothesized that, in undifferentiated cells, genes that encode lineage-specific factors would be found in nuclear peripheral heterochromatin and would be released from the nuclear periphery upon differentiation. We examined the nuclear localization of individual loci that are differentially marked by H3K9me2 according to the differentiation conditions. Myocyte enhancer factor 2c (*Mef2c*) is a transcription factor that is involved in neurogenesis (Leifer et al., 1993) as well as cardiogenesis (Lin et al., 1997). H3K9me2 ChIP-seq data indicate that the *Mef2c* locus is H3K9me2-marked in undifferentiated P19 cells and in D3 DMSO-differentiated cells, but H3K9me2 is reduced at the *Mef2c* locus in D3 RA-differentiated cells (average H3-normalized H3K9me2 counts per kb: undifferentiated=19.6, D3 RA-treated=−16.2, D3 DMSO-treated=16.2). We performed high-resolution 3D immunofluorescent *in situ* hybridization (immuno-FISH) (Poleshko et al., 2017) to assess the position of the *Mef2c* locus and to quantify the 3D distance between the locus and the nuclear periphery. *Mef2c*-specific DNA FISH probes were used to visualize the locus relative to the nuclear lamina (LaminB immunofluorescence). Given that DMSO-treatment results in efficient differentiation of only a subset of cells at D3 (Fig. 1D,E), we included immunofluorescence of Oct4 in the immuno-FISH protocol and focused on Oct4<sup>+</sup> cells in the D3 DMSO-treated analysis. Through high-resolution 3D immuno-FISH, we verified that the *Mef2c* locus was positioned at the nuclear periphery in both undifferentiated P19 cells (Oct4<sup>+</sup>) and D3 DMSO-treated Oct4<sup>+</sup> cells, but was repositioned away from the nuclear periphery in D3 RA-treated cells (Oct4<sup>−</sup>) (Fig. 3E,F). We quantified

the 3D distance to the nuclear lamina for each allele in each condition and observed a statistically significant difference between undifferentiated and D3 RA-treated cells as well as D3 DMSO-treated Oct4<sup>−</sup> cells compared with D3 RA-treated cells (Fig. 3F). For each condition, we also scored the number of alleles (0, 1, or 2) at the nuclear periphery in each cell and found that only D3 RA-treated samples had a majority of cells with at least one allele repositioned away from the nuclear periphery (Fig. 3G). These data are consistent with our H3K9me2 ChIP-seq findings and suggest that the release of the *Mef2c* locus from the nuclear periphery is specific to the neuronal cell-fate choice at D3 of RA-induced differentiation.

Another gene locus that displayed lineage-specific changes in H3K9me2 is myocardin (*Myocd*), which is a master regulator of cardiomyocytes and cardiac smooth muscle (Li et al., 2003; Wang et al., 2001). Comparison of the H3K9me2 ChIP-seq signal at the *Myocd* locus in undifferentiated P19 cells with that found at *Myocd* in D3 DMSO-treated cells revealed specific loss of H3K9me2 in D3 DMSO-treated, but not in D3 RA-treated samples (average H3-normalized H3K9me2 counts per kb: undifferentiated=15.3, D3 RA-treated=21.3, D3 DMSO-treated=−4.3). Consistent with the H3K9me2 ChIP-seq data, observations of the *Myocd* genomic locus by 3D immuno-FISH revealed that this locus was positioned at the nuclear periphery in undifferentiated P19 cells but localized to the nuclear interior in D3 DMSO-treated Oct4<sup>−</sup> cells (Fig. 3H–J). In D3 RA-treated samples, the majority of the *Myocd* locus remained at the nuclear periphery (Fig. 3I,J). These results indicate that release of the *Myocd* locus from the nuclear periphery is specific to the D3 DMSO-induced cardiomyocyte lineage.

#### Loss of locus-specific H3K9me2 mark correlates with transcriptional activation for a subset of genes

Several studies have shown that positioning of genomic loci at the nuclear periphery is correlated with transcriptional repression (Peric-Hupkes et al., 2010; Robson et al., 2016) and inhibition of G9a, the histone methyl-transferase that is responsible for H3K9 dimethylation, which results in upregulated expression of lamin-associated genes (Yokochi et al., 2009). We therefore asked whether those genes that have changes in H3K9me2 and nuclear localization also vary in transcriptional activity during lineage specification.

We examined genome-wide changes in gene expression during lineage-specific H3K9me2 reorganization through RNA-seq analysis of undifferentiated, RA- and DMSO-treated P19 cells. Across all treatment conditions, genes that are found within H3K9me2 domains have significantly lower gene expression compared with those outside of H3K9me2 domains (Fig. S4A,  $P<2.2\times10^{-16}$  Mann–Whitney *U*-test). We assessed the connection between transcriptional activity and the changes in nuclear peripheral positioning that occurred during our differentiation protocol by examining the expression level of genes that have reduced H3K9me2 specifically in D3 RA-treated or D3 DMSO-treated samples relative to undifferentiated P19 cells. Although most genes that show an RA treatment-specific reduction in H3K9me2 domain residency had no corresponding change in gene expression (69.9%), a subset of genes (27.6%), including *Mef2c*, was transcriptionally upregulated in D3 RA (Fig. 4A, dots sized by quartile rank in undifferentiated RNA-seq; Table S8). This suggests that the release of a significant number of genes from the repressive environment of the nuclear periphery, which occurred during RA differentiation, was associated with upregulation of gene expression in D3 RA-treated P19 cells. We did not observe any significant number of genes that show DMSO-specific reduction of H3K9me2 to be transcriptionally upregulated in D3 DMSO (Fig. 4B; Table S9).

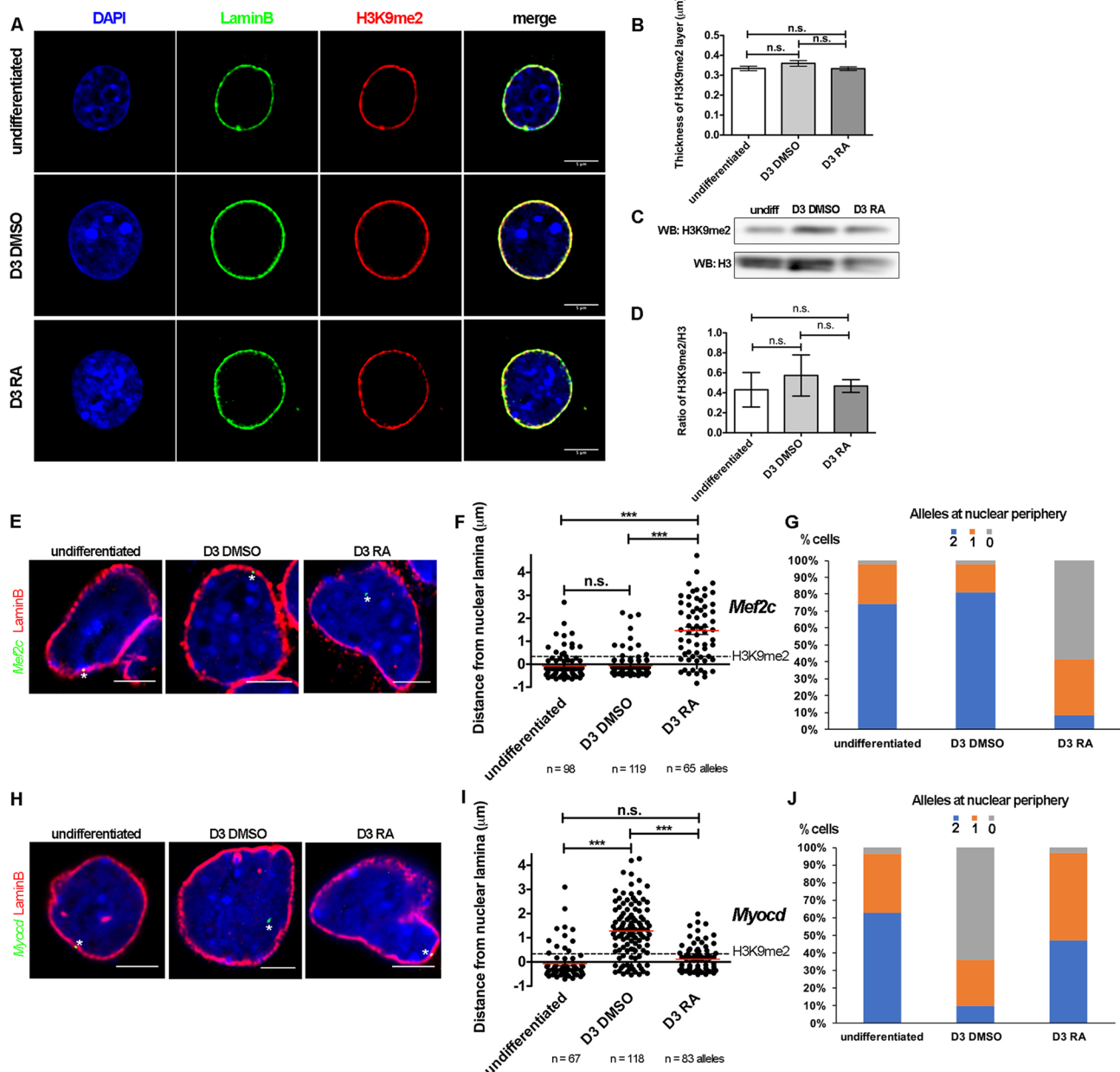


**Fig. 3. Lineage-specific master regulators *Mef2c* and *Myoecd* are specifically repositioned from nuclear peripheral heterochromatin during cell-fate choice.** (A) Immunofluorescence of H3K9me2 and LaminB reveals nuclear peripheral heterochromatin in undifferentiated, D3 DMSO- and D3 RA-treated P19 cells. (B) Quantification of H3K9me2 layer thickness. One-way ANOVA test.  $n=30$  measurements per condition. Error bars indicate s.e.m. (C) Representative western blot of H3K9me2 and H3 in nuclear lysates of undifferentiated, D3 DMSO- and D3 RA-treated P19 cells. (D) Quantification of H3K9me2 (normalized by H3) western blot levels. One-way ANOVA test.  $n=3$  biological replicates. (E) High-resolution 3D immuno-FISH reveals that the *Mef2c* genomic locus is specifically released from the nuclear periphery in D3 RA-treated, but not in undifferentiated or D3 DMSO-treated cells. Representative single confocal z-slice of immuno-FISH of indicated loci in each cell type immunostained with LaminB. (F) Quantification of 3D distance between *Mef2c* locus and the nuclear periphery. One-way ANOVA test. \*\*\* $P<0.001$ . Dotted line represents the thickness of H3K9me2; red line indicates mean;  $n$ , number of alleles counted per condition. For the D3 DMSO-treated condition, Oct4<sup>-</sup> cells were quantified. (G) Percentage of cells with 0, 1 or 2 alleles of *Mef2c* at the nuclear periphery. Average number of cells is 31 cells per condition. (H) High-resolution 3D immuno-FISH reveals that the *Myoecd* genomic locus is specifically released from the nuclear periphery in D3 DMSO-treated, but not in undifferentiated or D3 RA-treated cells. Representative single confocal z-slice of immuno-FISH of indicated loci in each cell type immunostained with LaminB. (I) Quantification of 3D distance between *Myoecd* locus and the nuclear periphery. One-way ANOVA test. \*\*\* $P<0.001$ . Dotted line represents the thickness of H3K9me2; red line indicates mean;  $n$ , number of alleles counted per condition. For the D3 DMSO-treated condition, Oct4<sup>-</sup> cells were quantified. (J) Percentage of cells with 0, 1 or 2 alleles of *Myoecd* at the nuclear periphery. Average number of cells is 36 cells per condition. n.s., not significant. Asterisks (E,H) highlight the position of the genomic locus. Scale bars: 5  $\mu\text{m}$  in A; 5  $\mu\text{m}$  in E,H.

To determine whether genes that were released from the nuclear periphery might be transcriptionally activated at a later stage of differentiation, we analyzed RNA-seq data from D6 RA-treated samples. We found no significant difference in

gene expression profiles for the same set of genes between D3 RA- and D6 RA-treated ( $P=0.295$ ,  $2\times 3$  Chi<sup>2</sup> test, Fig. 4C; Table S10). Similarly, we found that most loci with DMSO-specific reduction in H3K9me2 according to ChIP-seq

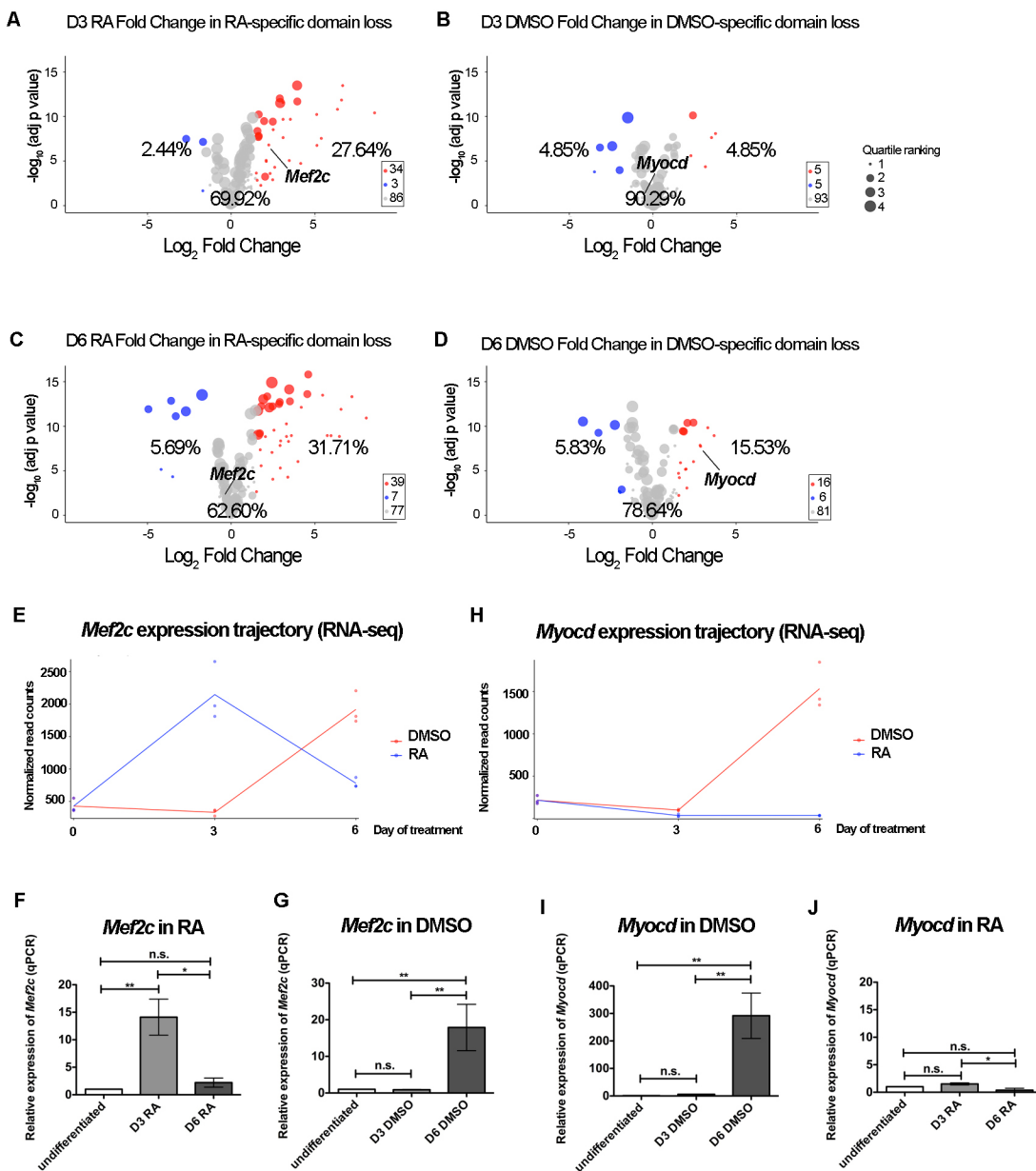


**Fig. 4. Loss of residency within H3K9me2 domains results in transcriptional activation for subset of genes.** (A) Volcano plot showing D3 RA RNA-seq expression profile of genes that lost residency within H3K9me2 domains specifically in D3 RA-treated cells. A substantial proportion of genes (23.93%) are transcriptionally upregulated when spatially repositioned from the nuclear periphery. Dots are sized by quartile ranking of expression in undifferentiated P19 cells. Red dots indicate significantly upregulated genes ( $\log_2$  fold change  $\geq 1.5$ ,  $P \leq 0.05$ ), blue dots indicate significantly downregulated genes ( $\log_2$  fold change  $\leq -1.5$ ,  $P \leq 0.05$ ), gray dots are non-significantly changed. Fold changes calculated for D3 RA-treated cells with respect to undifferentiated cells. (B) Volcano plot showing D3 DMSO RNA-seq expression profile of genes that lost residency within H3K9me2 domains specifically in D3 DMSO-treated cells. Most genes that repositioned away from the nuclear periphery in D3 DMSO-treated cells did not have associated transcriptional changes. Fold changes calculated for D3 DMSO-treated cells with respect to undifferentiated cells. (C) Volcano plot showing D6 RA RNA-seq expression profile of genes that lost residency within H3K9me2 domains specifically in D3 RA-treated cells. Fold changes calculated for D6 RA-treated cells with respect to undifferentiated cells. (D) Volcano plot showing D6 DMSO RNA-seq expression profile of genes that lost residency within H3K9me2 domains specifically in D3 DMSO-treated cells. Fold changes calculated for D6 DMSO-treated cells with respect to undifferentiated cells. (E) *Mef2c* expression trajectory across day 3 (D3) and day 6 (D6) of treatment based on RNA-seq data. (F,G) Relative gene expression levels of *Mef2c* across RA or DMSO differentiation by RT-qPCR. One-way ANOVA. \* $P < 0.05$ , \*\* $P < 0.01$ ; n=3–5 biological replicates. (H) *Myoecd* expression trajectory across day 3 (D3) and day 6 (D6) of treatment based on RNA-seq data. (I,J) Relative gene expression levels of *Myoecd* across DMSO or RA differentiation by RT-qPCR. One-way ANOVA. \* $P < 0.05$ , \*\* $P < 0.01$ . n=3–5 biological replicates. n.s. not significant.

analysis showed little significant difference in gene expression when assayed at D3- or D6- DMSO treatment (Fig. 4D,  $P=0.0354$ ,  $2\times 3$  Chi<sup>2</sup> test; Table S11). This suggests that most genes that were released at D3 were not transcriptionally upregulated by D6 of differentiation, though we cannot rule out that they would be upregulated at later time points.

According to our RNA-seq analysis, expression of *Mef2c* is ~fourfold higher in D3 RA-treated cells than in undifferentiated P19 cells (Fig. 4E), which is consistent with both its reduction in H3K9me2 signal and localization change from the nuclear periphery towards the nuclear interior (Fig. 3F). By day 6 of RA treatment, however, *Mef2c* expression is relatively diminished (Fig. 4C,E). In

addition to neurogenesis, *Mef2c* is also known to play a role in cardiac and skeletal muscle development (Lin et al., 1997) and has been previously shown to be transcriptionally upregulated in P19 cells by day 6 of DMSO treatment (Grépin et al., 1997; Skerjanc et al., 1998). Our RNA-seq results confirmed that *Mef2c* is expressed in D6 DMSO (Fig. 4E). We further validated these results with RT-qPCR (Fig. 4F,G). *Mef2c* expression was upregulated in D3 RA, but not in D6 RA samples (Fig. 4F), whereas DMSO treatment led to *Mef2c* expression being unchanged in D3 DMSO samples, but dramatically upregulated at D6 DMSO (Fig. 4G). The expression data for *Mef2c* correlates with nuclear localization and demonstrates a link between transcriptional activity and spatial positioning of a genomic locus in the nucleus. Notably, this illustrates lineage-specific modification of the H3K9me2 mark and its association with gene expression during cell-fate specification.

Given the less efficient differentiation induced by DMSO at D3, the lack of transcriptional upregulation of most genes in D3 DMSO might be because of the heterogeneity of this population of cells. *Myoecd* is an example of a locus that was released from the nuclear periphery specifically in the D3 DMSO-treated cells. *Myoecd* was transcriptionally unchanged at D3 DMSO treatment, but was dramatically upregulated in D6 DMSO cells (Fig. 4B,D,H). This was verified through RT-qPCR analysis (Fig. 4I). Notably, this upregulation is specific to D6 DMSO and is not found in RA differentiation (Fig. 4H,J). Thus, *Myoecd* is an example of a gene that is first released from the nuclear periphery at D3 DMSO, before the observed transcriptional upregulation at D6 DMSO. This provides evidence for genomic loci to be repositioned away from the nuclear periphery during early stages of differentiation before transcriptional activation at later stages of differentiation. Taken together, this demonstrates that the local reorganization of H3K9me2-marked nuclear peripheral heterochromatin is lineage-specific, but is not always associated with changes in transcriptional activity.

## DISCUSSION

We report that H3K9me2-marked nuclear peripheral heterochromatin undergoes dynamic local reorganization during differentiation and that the loss of H3K9me2-marked domains displays lineage specificity. These lineage-specific regions contain genes that are functionally important for the future fate of the cell. Using high-resolution 3D immuno-FISH, we confirm that the changes in H3K9me2 domains as determined by ChIP-seq are consistent with spatial repositioning of genomic loci (*Mef2c*, *Myoecd*) with respect to the nuclear periphery. Most genes that are released from the nuclear periphery do not have transcriptional changes, but a subset of genes has associated transcriptional upregulation. We provide evidence that the dynamic local reorganization of H3K9me2-marked nuclear peripheral heterochromatin is lineage specific.

Understanding the mechanisms that drive cell-fate specification is at the heart of developmental biology and a number of studies have described the transcriptional changes that accompany cell fate choice. In addition, the three-dimensional nuclear architecture and its impact on the localization of relevant gene loci within different compartments of the nucleus should be recognized and examined in the context of cell-fate specification. In this study, by demonstrating that there is lineage-specific reorganization of H3K9me2-marked nuclear peripheral heterochromatin during cell-fate choice, we provide evidence that the same multipotent progenitor cell reorganizes its peripheral heterochromatin specifically according to the distinct cell fate it is adopting.

## Spatial regulation of transcriptional activation

We found that loss of the H3K9me2 mark in specific domains corresponds to repositioning of genomic loci away from the nuclear periphery, suggesting that H3K9me2 ChIP-seq accurately predicts spatial positioning of genomic regions within nuclear peripheral heterochromatin. In *Caenorhabditis elegans*, MET-2 and SET-25 (orthologs of G9a and SetDB1), enzymes that promote mono-/di-methylation or tri-methylation of lysine 9 on histone 3 (H3K9), respectively, are necessary for anchoring chromatin to the nuclear lamina and for transcriptional repression of heterochromatin (Gonzalez-Sandoval and Gasser, 2016; Towbin et al., 2012). Loss of SET-25 and MET-2 leads to loss of H3K9me1/2/3, transcriptional de-repression, and subsequent detachment of chromosomal regions from the nuclear lamina, which is generally consistent with our observations.

We found that the release of genomic loci from the nuclear periphery is not always concomitant with transcriptional activation, but a subset of released genes is transcriptionally upregulated. Consistent with this, there was no strong genome-wide correlation of gene detachment and upregulation in MET-2/SET-25 mutants, though a subset of genes that detach from the nuclear lamina was strongly upregulated (Gonzalez-Sandoval et al., 2015; Towbin et al., 2012). We interpret these findings to suggest that detachment from the nuclear periphery equates to competence for gene activation, but that additional transcriptional activation events are necessary for gene transcription subsequent to or simultaneous with detachment.

A recent study identified CEC-4 in *C. elegans* as a protein that specifically recognizes H3K9me2 and mediates the perinuclear localization of heterochromatin independent of lamin (Gonzalez-Sandoval et al., 2015). Loss of CEC-4 resulted in repositioning of loci away from the nuclear periphery, but these genes remained transcriptionally repressed and there was no global derepression observed (Gonzalez-Sandoval et al., 2015). This suggests that the spatial positioning of a locus can be uncoupled from transcriptional control (Gonzalez-Sandoval and Gasser, 2016). Indeed, it has been reported that chromatin decondensation is sufficient to reposition genomic loci away from nuclear periphery in mESCs without transcriptional activation (Therizols et al., 2014). This underscores the importance of defining the genome-wide H3K9me2 distribution to inform both the spatial positioning and repressive potential of genomic loci. In our study, we found that the loss of H3K9me2-marked domains accurately predicts spatial repositioning away from the nuclear periphery. We propose that this spatial repositioning increases the accessibility of the genomic loci for subsequent activation by enhancers or transcription factors during appropriate stages of lineage specification.

## Spatial and temporal regulation of master regulators *Mef2c* and *Myoecd*

*Mef2c* encodes a master regulator transcription factor that has been reported to be involved in neurogenesis (Leifer et al., 1993) and cardiogenesis (Lin et al., 1997). However, it remains unclear how the same transcription factor can be involved in two distinct lineage commitments. Interestingly, we observed that the timing of repositioning of the *Mef2c* locus from nuclear peripheral heterochromatin is highly specific to the fate that a cell adopts. We found that *Mef2c* is repositioned away from the nuclear periphery in D3 RA-induced early neurogenic differentiation and associated with transcriptional upregulation for neurogenesis. Conversely, we found that *Mef2c* remains at the nuclear periphery in D3 DMSO-induced early cardiogenic differentiation, but is

transcriptionally upregulated only later at D6 after DMSO-induced cardiac differentiation. Consistent with this, a previous study that described cardiogenesis in P19 cells reported that *Mef2c* is upregulated at D6 DMSO and, together with Nkx2-5, initiates cardiogenesis (Skerjanc et al., 1998). This suggests that the same genomic locus (*Mef2c*) can be repositioned away from the nuclear periphery at lineage-specific time points during cell-fate choice. This would provide an additional layer of spatial regulation of accessibility for the same transcription factor that is involved in two distinct cell fates.

*Myocd* encodes a master regulator for cardiac and smooth muscle (Li et al., 2003; Wang et al., 2001). We found that *Myocd* was released at D3 DMSO-induced early cardiogenic differentiation, but was not transcriptionally upregulated until D6 DMSO-treatment. This was not unexpected as *Myocd* has previously been reported to be expressed at D6 DMSO together with *Mef2c* in P19 cells, and to be required for cardiogenesis (Ueyama et al., 2003). Indeed, *Mef2c* has been shown to directly activate a distal *Myocd* enhancer during cardiovascular development (Creemers et al., 2006). Consistent with this result, we found that the *Myocd* locus is released from the periphery at D3 DMSO, but the expression of both *Myocd* and *Mef2c* are highly upregulated only at D6 DMSO. This suggests that the genomic locus (*Myocd*) can first be repositioned away from the nuclear periphery before transcriptional activation at later stages of development when other appropriate transcriptional activators (e.g. *Mef2c*) are expressed.

Taken together, we find that the spatial repositioning of genomic loci, such as master regulators *Mef2c* and *Myocd*, away from the nuclear periphery is tightly controlled during cell-fate decisions and the timing of release is tightly regulated in the process of lineage specification. Our data are consistent with a model in which lineage-specific master regulators positioned at the nuclear periphery in undifferentiated cells are specifically released and accessible for transcriptional activation during cell-fate determination. The dynamic reorganization of nuclear peripheral heterochromatin and H3K9me2 domains provides an additional layer of spatial regulation of transcription during lineage specification. Future studies will aim to uncover the molecular mechanisms that regulate lineage-specific reorganization of nuclear peripheral heterochromatin.

## MATERIALS AND METHODS

### Cell culture

P19 cells were obtained from ATCC (CRL-1825) and maintained at low confluence in  $\alpha$ -Minimum Essential Media ( $\alpha$ -MEM, 12571048, Invitrogen) supplemented with 10% fetal bovine serum (charcoal stripped FBS, F6765 Sigma-Aldrich) and 1% penicillin/streptavidin. P19 cells were differentiated in 1  $\mu$ M RA (R2625, Sigma-Aldrich) or in 1% DMSO (D2650, Sigma-Aldrich) by forming embryoid bodies (EBs) for 2 days in bacteriological petri dishes, before transferring to T75 cell culture flasks and replacing with maintenance media.

### Western blots

Protein lysates were run on 4%-12% NuPAGE Bis-Tris protein gels (NP0335, Invitrogen) and blots were probed with anti-H3K9me2 (1:2500, ab1220, Abcam), anti-H3 (1:2000, ab1791, Abcam), anti-Gata4 (1  $\mu$ g/ml, ab84593, Abcam), anti-EphA3 (1:1000, sc-514209, Santa Cruz Biotechnology), anti-Pou5f1 (1:1000, ab19857, Abcam), anti-Gapdh (1:1000, 2118S, Cell Signaling Technology) according to manufacturer's instructions. Secondary antibodies used were: anti-rabbit IgG conjugated HRP (1:2000, 7074S, Cell Signaling Technology) or anti-mouse IgG conjugated HRP (1:5000, 7076S, Cell Signaling Technology). ECL Prime Western Blotting System (RPN2232, GE Healthcare) and Amersham Imager 600 (GE Healthcare) were used for visualization and imaging.

### ChIP-seq library preparation

ChIP was performed similar to previously described (Poleshko et al., 2017). Briefly, P19 cells were resuspended and crosslinked in media with 1% methanol-free formaldehyde (Thermo Fisher Scientific) for 10 min at room temperature (rtp) with gentle rotation. Crosslinking was quenched with addition of glycine (125 mM final concentration) and incubated at rtp for 5 min with gentle rotation. Cells were pelleted by centrifugation (300 g for 3.5 min rtp) and resuspended in PBS, transferred to Eppendorf tubes and pellets were obtained by centrifugation (300 g for 3.5 min). Supernatant was discarded and pellets were flash frozen on dry ice and stored at -80°C.

For each ChIP sample, 50  $\mu$ l of Dynabeads Protein G for Immunoprecipitation (10004D, Invitrogen) was washed in block buffer [0.5% bovine serum albumin (BSA) in PBS] 3 $\times$  and beads were resuspended in 500  $\mu$ l block buffer with 5  $\mu$ g antibody (anti-H3K9me2, ab1220, Abcam; anti-H3, ab1791, Abcam) and incubated at 4°C with rotation for 6 h. Another 50  $\mu$ l of Dynabeads Protein G per ChIP sample was washed in block buffer 3 $\times$ , resuspended in 500  $\mu$ l block buffer and set aside for pre-clearing of sonicated chromatin.

To obtain nuclei from the frozen cross-linked pellets, cells were resuspended in cold Cell Lysis Buffer 1 (50 mM HEPES-KOH, 140 mM NaCl, 1 mM EDTA, 10% glycerol, 0.5% NP-40, 0.25% Triton X-100, fresh protease inhibitors) and rotated at 4°C for 10 min, followed by centrifugation (300 g for 4 min). Supernatant was discarded and pellet was resuspended in cold Cell Lysis Buffer 2 (10 mM Tris-HCl, 200 mM NaCl, 1 mM EDTA, 0.5 mM EGTA, fresh protease inhibitors) and rotated for 10 min at rtp. Pellet was obtained by centrifugation (300 g for 4 min) and resuspended in 1 ml cold Lysis Buffer 3 (10 mM Tris-HCl, 100 mM NaCl, 1 mM EDTA, 0.5 mM EGTA, 0.1% Na-deoxycholate, 0.5% N-laurylsarcosine, fresh protease inhibitors) and transferred to a pre-chilled 1 ml Covaris AFA tube. Samples (10 million cells per tube) were sonicated for 10 min at 4°C in a sonicator (Covaris S220). Sonicated lysate was transferred to Eppendorf LoBind tubes and Triton X-100 added (to a final concentration of 1%). Samples were centrifuged at maximum speed for 10 min at 4°C and supernatant was transferred to 500  $\mu$ l pre-clearing beads and rotated for 2 h at 4°C. Pre-cleared sonicated chromatin was collected as supernatant by centrifugation at maximum speed for 10 min at 4°C. Quantification of DNA was performed using Qubit dsDNA HS assay kit (Q32854, Invitrogen). Antibody-conjugated beads were washed thrice in block buffer and resuspended in 100  $\mu$ l of block buffer. Each ChIP sample had 15  $\mu$ g of pre-cleared sonicated chromatin added to antibody-conjugated beads and incubated with rotation at 4°C overnight. We set aside 1.5  $\mu$ g of sonicated chromatin per sample for input.

On the second day, beads were collected with magnetic holder (Dynamag-2 magnet, Thermo Fisher Scientific) and washed 5 $\times$  in 1 ml RIPA wash buffer (50 mM HEPES-KOH, 500 mM LiCl, 1 mM EDTA, 1% NP-40, 0.7% Na-deoxycholate) with 5 min rotation at rtp per wash. Beads were washed in 1 ml final ChIP wash buffer [50 mM NaCl, 1× Tris-EDTA buffer (TE)] and 10% aliquot set aside for ChIP-western blotting before final resuspension in ChIP elution buffer (10 mM EDTA, 50 mM Tris-HCl, 1% SDS) and eluted at 65°C for 30 min. Around 10% of beads/input were set aside for ChIP-western blotting with anti-H3K9me2 antibody/anti-H3 antibody to ensure that there was effective immunoprecipitation of target antibody. Eluted ChIP DNA or thawed input DNA was transferred to a new LoBind tube and incubated at 65°C overnight to reverse crosslinks.

On the third day, 200  $\mu$ l of 1× TE was added to the reverse crosslinked ChIP DNA and RNase treated (final concentration 0.2 mg/ml, 1010969001, Roche) at 37°C for 2 h, and Proteinase K treated (final concentration 0.2 mg/ml, CB3210-5, Denville Scientific) at 55°C for 2 h. ChIP and input DNA were purified through phenol:chloroform extraction and resuspended in 10 mM Tris-HCl (pH 8). Quantification of ChIP and input DNA was performed using Qubit dsDNA HS assay kit. ChIP-seq library preparation used 250 ng of ChIP or input DNA for the Next Ultra II DNA Library preparation kit for Illumina (E7645S, New England Biolabs) and NEBNext multiplex oligos for Illumina (dual index primers set I, E7600S, New England Biolabs) according to the manufacturer's instructions. The quality of individual ChIP-seq libraries was assessed using Bioanalyzer (High Sensitivity DNA kit, 5067-4626, Agilent) and quantified by qPCR using Kapa Library Quantification Kit (KK4835, Kapa Biosystems). Libraries

were normalized and pooled for multiplex sequencing, re-quantified and sequenced on Nextseq500 platform (75 bp, single end, Illumina).

### ChIP-seq analysis

Sequencing reads were aligned to genome assembly (NCBI37/mm9) using Bowtie2 (version 2.2.9) with default parameters and ‘–local’ to allow soft clipping of ends. Alignments were further processed by SAMtools (version 0.1.19) to remove low quality alignments (‘-q 10’) and read duplicates (‘rmdup -s’). Individual biological replicates had high correlation (Fig. S3A) and were merged using SAMtools. Each individual sample had an average of ~37.1 million reads (Table S3).

H3K9me2 domains for individual and pooled libraries were called using EDD (version 1.1.18) (Lund et al., 2014), which is ideal for the discovery of broad enrichment domains from ChIP-seq data. We used the following parameters ‘–bin-size auto –gap-penalty 3 –fdr 0.05’ with H3K9me2 ChIP-seq as ‘ChIP’ and H3 ChIP-seq as ‘input’ to define H3K9me2 domains. Blacklist regions from ENCODE mm9 and default EDD mm9 blacklist regions were used and the required fraction of uninformative bins is 0.97.

The visualization track of the individual library was generated using bedtools, for which the genome coverage was normalized to 1 million reads per library. Tracks of log2-fold change between H3K9me2 and H3 ChIP were generated using deepTools (version 3.0.1, ‘bigwigCompare –pseudocount=0.00001 –binSize=100’). The log2-fold change tracks were further quantile normalized using bwtool (version 1.0, ‘summary –binSize=100’) and R package preprocessCore (Bioconductor). A similar track generation approach was performed for merged replicates.

Spearman correlations between ChIP-seq libraries over the whole genome were computed using 10 kb bins and plotted using deepTools (‘multiBigwigSummary’ and ‘plotCorrelation’). Metaplots of ChIP signal flanking differentially bound sites were also generated using deepTools (‘computeMatrix’ and ‘plotHeatmap’).

EDD called H3K9me2 domains were used as input into bedtools multiinter, which allowed identification of shared and unique domains of D0, DMSO and RA treatments. ENSEMBL mm9 gtf file was parsed with GTFtools (Li, 2018preprint) to create a gene start and stop coordinate file. Bedtools (version v2.27.1) intersect was used to find overlaps between gene coordinates and H3K9me2 domains. For a gene to be considered overlapping, 75% of the total gene length must lie within an H3K9me2 domain(s). Gene intersection output was used to extract lists of genes (Tables S5-S7) that are associated with shared and unique H3K9me2 domain subsets.

To obtain H3-normalized H3K9me2 counts per kb, we subtracted H3 ChIP-seq reads from H3K9me2 ChIP-seq reads across the region that covered the gene body with +5 kb extensions on both ends. The H3-normalized counts were then normalized by gene length per kb.

### RNA isolation and preparation

Total RNA was isolated in Trizol (15596026, Ambion) and purified using RNeasy mini columns (74104, Qiagen) according to the manufacturer’s instructions. RNA was digested with DNase I (AM2238, Ambion) at 37°C for 30 min and heat inactivated at 70°C for 5 min before a second round of RNeasy cleanup. cDNA was synthesized using oligo dT primers with SuperScript III reverse transcriptase (18080044, Invitrogen). RT-qPCR were performed in triplicate with PowerSYBR Green PCR Master Mix (4367659, Applied Biosystems) on StepOnePlus Real-Time PCR System (43776600, Applied Biosystems). *Gapdh* was used as a housekeeping normalization control. The sequence of primers used for RT-qPCR are found in Table S4.

### RNA-seq analysis

RNA-seq libraries were prepared using Truseq Stranded Total RNA Library Prep Kit with Ribo-Zero Human/Mouse/Rat Set A (RS-122-2201, Illumina) according to the manufacturer’s instructions and sequenced using NextSeq 500 platform (75 bp, single-end, Illumina). Fastq files were assessed for quality using the FastQC (version 0.11.2) program and aligned to the mouse genome assembly NCBI37/mm9 using STAR (version 2.6.0c) (Dobin et al., 2012). Unmapped reads, non-primary alignments and alignments with a MAPQ score of <10 were filtered with SAMtools.

### Gene ontology

DAVID Gene Ontology (GO) (Huang et al., 2009) v6.8 was used for Gene Ontology (Biological Process) analysis and only terms with  $P<0.05$  and false discovery rate (FDR)<0.05 were considered for enrichment.

### Differential expression analysis

Rsubread (Liao et al., 2013) package’s featureCounts function was used to count the number of uniquely mapping reads per gene using Ensembl v.67 mm9 gene annotation file. For differential gene expression analysis, genes with <1 count per million (CPM) in less than 25% of samples were removed from differential expression analysis. Limma (Ritchie et al., 2015) voom function was used to log transform and quantile normalize the CPM matrix. Limma was used with a linear model to perform differential gene expression analysis with adjusted  $P$ -values for multiple comparisons using the Benjamini–Hochberg procedure (Benjamini and Hochberg, 1995). Cutoffs of  $FDR\leq 0.05$  and fold change  $\geq 1.5$  or  $\leq -1.5$  were used for significantly upregulated or downregulated genes. Genes that had at least 75% overlap with H3K9me2 domains were considered to be found within domains and were used for downstream analysis. The Mann–Whitney  $U$ -test was performed in R. Heatmaps were generated using R.

### Volcano plots

Volcano plots of protein coding genes that are associated with RA-specific loss or DMSO-specific loss of H3K9me2 domains were visualized using R’s ggplot2 (version 2.2.1) package and show upregulated (red), downregulated (blue) and not differentially expressed (gray) genes, based on adjusted  $P$ -value  $\leq 0.05$  and log2-fold change thresholds of  $\pm 1.5$ , respectively. Fold changes of genes used in Fig. 4A-D are found in Tables S8-S11.

### Boxplots

To analyze gene expression of all genes associated with H3K9me2 domains, undifferentiated and D3 RNA-seq count data were normalized similar to the undifferentiated, D3 and D6 RNA-seq differential expression analysis except lowly expressed genes were not removed. All non-protein coding genes were removed. Gene lengths were calculated using GTFTools (Li, 2018 preprint), outputting the maximum transcript length for each gene. Reads per kilobase of transcript per million mapped reads values were then generated by normalizing CPM values to gene length. Using the unique and shared H3K9me2 domain gene lists for each treatment, R (version 3.4.3) and ggplot2 (version 2.2.1) were used to construct boxplots of gene expression package.

### Immunofluorescence and DNA FISH

P19 cells were grown on glass coverslips (#1, 22×22 mm, 102222, Thermo Fisher Scientific) and fixed in 2% paraformaldehyde (PFA) for 10 min at rtp and washed thrice in PBS. Cells were permeabilized in 0.5% Triton X-100 for 10 min at rtp, washed thrice in PBS and incubated in block solution (1% BSA, PBS, 0.1% Triton X-100, 0.05% Tween 20) for 1 h at rtp. Cells were incubated with primary antibody for 1 h, washed thrice in 1× PBST (PBS, 0.05% Tween 20) and incubated with secondary antibody for 1 h at rtp. Cells were washed in twice in PBS for 5 min each and counterstained with DAPI (D9542, Sigma-Aldrich) for 10 min at rtp. Cells were washed in PBS twice before mounting on glass slides with mounting medium (Vectashield). Primary antibodies used were anti-LaminB1 (1:500, sc-374015, Santa Cruz Biotechnology), anti-LaminB1 (1:500, sc-6216, Santa Cruz Biotechnology), anti-H3K9me2 (1:500, 39239, Active Motif), anti-Oct4 (1:500, ab19857, Abcam) and secondary antibodies used include donkey anti-rabbit Alexa 568 (1:500, A10042, Invitrogen), donkey anti-mouse Alexa 568 (1:500, A10037, Invitrogen), donkey anti-goat Alexa 488 (1:500, A11055, Invitrogen) or goat anti-rabbit Alexa 568 (1:500, A11011, Invitrogen). Cells were either imaged at this stage or processed further for DNA FISH, in which case cells were post-fixed in 2% PFA for 10 min at rtp and permeabilized with ice cold 0.7% Triton X-100/0.1 M HCl for 10 min. Cells were denatured at 75°C for 30 min in 50% formamide/2× saline-sodium citrate buffer (SSC) and transferred to ice cold 2× SSC, before hybridization with labeled probe. Probes were labeled with green dUTP using Nick Translation Kit (32-801300, Abbott Laboratories) and denatured for 30 min at 37°C and 10 min at 75°C immediately before hybridization.

BAC DNA clones (Thermo Fisher Scientific) used were *Mef2c* (RP23-187H18) and *Myocd* (RP23-379F14). The immuno-FISH protocol contains a denaturation step of 75°C for 30 min, which is essential to allow the cellular DNA to be denatured before hybridization with the DNA FISH probes. This time-critical step is carefully administered and we do not observe fragmented nuclei or compromised nuclear integrity after this step. The immunostaining in some cells may be slightly disrupted after the denaturation step. If the cells displayed compromised nuclear integrity, they were excluded from analysis.

### Flow cytometry

Cells were counted and aliquoted at  $5 \times 10^5$  per fluorescence-activated cell sorting (FACS) tube. Cells were washed once in FACS wash buffer (2% FBS in PBS), collected as a pellet by centrifugation at 500 g for 10 min and resuspended in 250 µl of Fixation/Permeabilization solution (BD Biosciences) to incubate for 20 min at 4°C. Cells were washed once in 1× Perm/Wash Buffer (BD Biosciences) and collected as a pellet by centrifugation (500 g for 10 min). Anti-Oct3/4 antibody conjugated to PE (560186, BD Pharmingen) was prepared in 20 µl of 1× Perm/Wash buffer and the cell pellet was resuspended in antibody solution to incubate for 30 min at 4°C in the dark. Cells were washed twice in 1× Perm/Wash buffer and resuspended in 200 µl 1× Perm/Wash buffer for flow cytometry (BD Accuri). Negative controls included non-stained cells and mouse isotype IgG1<sub>k</sub> conjugated to PE (555749, BD Pharmingen)-stained cells.

### Image analysis and quantification

All confocal images were taken on laser scanning confocal microscope Leica 3X STED from the University of Pennsylvania Cell and Developmental Biology (CDB) Microscopy Core. Confocal 3D images were taken using a z-step size of 0.04 µm with a range of 80–200 z-slices per cell. Images were deconvoluted using Huygens Professional (Scientific Volume Imaging) and 3D reconstructions were performed on Imaris software 7.4 (Bitplane). Measurements of 3D distance from the center of each DNA FISH spot to the nuclear lamina surface are as previously described (Poleshko et al., 2017). In brief, the DNA FISH dots are generated using the spots tool at its intensity center of mass with a 300 nm diameter. The lamin surface and DAPI surface are generated using the surface tool and generate a 3D spheroid structure based on the entirety of confocal z-stacks that have a resolution of 0.04 µm (x,y,z). As the cells are allowed to attach to the glass coverslip, the nucleus is not a perfect sphere but rather more spheroid in shape. Spots that are embedded within the nuclear lamina return negative distances. For calculating the percentages of cells with 0, 1 or 2 alleles in Fig. 3G,J, only cells in which both alleles were visible by immuno-FISH were included for quantification. All statistical testing for one-way analysis of variance (ANOVA) with post hoc Tukey tests were performed using Prism 5 (Graphpad).

### Acknowledgements

We thank Penn Epigenetics Institute and the University of Pennsylvania CDB Microscopy Core for use of Next Generation Sequencing equipment and confocal microscopes, respectively.

### Competing interests

The authors declare no competing or financial interests.

### Author contributions

Conceptualization: K.S., R.J., C.L.S., J.A.E.; Methodology: K.S., Y.L.; Software: Y.L., J.R.; Validation: K.S., J.R., C.L.S.; Formal analysis: K.S., Y.L., J.R.; Investigation: K.S.; Resources: Y.L.; Data curation: K.S., Y.L., J.R.; Writing - original draft: K.S., C.L.S., J.A.E.; Writing - review & editing: K.S., R.J., C.L.S., J.A.E.; Visualization: K.S., Y.L., J.R., C.L.S.; Supervision: R.J., C.L.S., J.A.E.; Project administration: C.L.S., J.A.E.; Funding acquisition: R.J., J.A.E.

### Funding

This work has been supported by the National Institutes of Health (R35 HL140018 to J.A.E., DP2 HL147123 to R.J.), the Cotswold Foundation (to J.A.E.), the W.W. Smith endowed chair (to J.A.E.), the Gilead Sciences Research Scholars Award (to R.J.), and the Burroughs Wellcome Fund Career Award for Medical Scientists (to R.J.). R.J. and J.A.E. received support from the National Science Foundation (CMMI-1548571). Deposited in PMC for release after 12 months.

### Data availability

The ChIP-seq and RNA-seq data reported in this study have been deposited in GEO under accession number GSE121314.

### Supplementary information

Supplementary information available online at <http://dev.biologists.org/lookup/doi/10.1242/dev.174078.supplemental>

### References

- Benjamini, Y. and Hochberg, Y. (1995). Controlling the false discovery rate: a practical and powerful approach to multiple testing. *J. R. Stat. Soc. Ser. B Methodol.* **57**, 289–300.
- Creemers, E. E., Sutherland, L. B., McAnalley, J., Richardson, J. A. and Olson, E. N. (2006). Myocardin is a direct transcriptional target of Mef2, Tead and Foxo proteins during cardiovascular development. *Development* **133**, 4245–4256.
- Dekker, J., Belmont, A. S., Guttman, M., Leshyk, V. O., Lis, J. T., Lomvardas, S., Mirny, L. A., O’Shea, C. C., Park, P. J., Ren, B. et al. (2017). The 4D nucleome project. *Nature* **549**, 219–226.
- Dobin, A., Davis, C. A., Schlesinger, F., Drenkow, J., Zaleski, C., Jha, S., Batut, P., Chaisson, M. and Gingeras, T. R. (2012). STAR: ultrafast universal RNA-seq aligner. *Bioinformatics* **29**, 15–21.
- Edwards, M. K., Harris, J. F. and McBurney, M. W. (1983). Induced muscle differentiation in an embryonal carcinoma cell line. *Mol. Cell. Biol.* **3**, 2280–2286.
- Gonzalez-Sandoval, A. and Gasser, S. M. (2016). On TADs and LADs: spatial control over gene expression. *Trends Genet.* **32**, 485–495.
- Gonzalez-Sandoval, A., Towbin, B. D., Kalck, V., Cabianca, D. S., Gaidatzis, D., Hauer, M. H., Geng, L., Wang, L., Yang, T., Wang, X. et al. (2015). Perinuclear anchoring of H3K9-methylated chromatin stabilizes induced cell fate in *C. elegans* embryos. *Cell* **163**, 1333–1347.
- Grépin, C., Nemer, G. and Nemer, M. (1997). Enhanced cardiogenesis in embryonic stem cells overexpressing the GATA-4 transcription factor. *Development* **124**, 2387–2395.
- Guelen, L., Pagie, L., Brasset, E., Meuleman, W., Faza, M. B., Talhout, W., Eussen, B. H., de Klein, A., Wessels, L., de Laat, W. et al. (2008). Domain organization of human chromosomes revealed by mapping of nuclear lamina interactions. *Nature* **453**, 948–951.
- Huang, D. W., Sherman, B. T. and Lempicki, R. A. (2009). Systematic and integrative analysis of large gene lists using DAVID bioinformatics resources. *Nat. Protoc.* **4**, 44–57.
- Jasmin, R. A., Spray, D. C., Campos de Carvalho, A. C. and Mendez-Otero, R. (2010). Chemical induction of cardiac differentiation in p19 embryonal carcinoma stem cells. *Stem Cells Dev.* **19**, 403–412.
- Jones-Villeneuve, E. M. (1982). Retinoic acid induces embryonal carcinoma cells to differentiate into neurons and glial cells. *J. Cell Biol.* **94**, 253–262.
- Kind, J., Pagie, L., Ortobozkoyun, H., Boyle, S. S., de Vries, S. S., Janssen, H., Amendola, M., Nolen, L. D., Bickmore, W. A. and van Steensel, B. (2013). Single-cell dynamics of genome-nuclear lamina interactions. *Cell* **153**, 178–192.
- Kohwi, M., Lupton, J. R., Lai, S.-L., Miller, M. R. and Doe, C. Q. (2013). Developmentally regulated subnuclear genome reorganization restricts neural progenitor competence in *Drosophila*. *Cell* **152**, 97–108.
- Leifer, D., Krainc, D., Yu, Y. T., McDermott, J., Breitbart, R. E., Heng, J., Neve, R. L., Kosofsky, B., Nadal-Ginard, B. and Lipton, S. A. (1993). MEF2C, a MADS/MEF2-family transcription factor expressed in a laminar distribution in cerebral cortex. *Proc. Natl. Acad. Sci. USA* **90**, 1546–1550.
- Li, H. (2018). GTFTools: a Python package for analyzing various modes of gene models. *bioRxiv*.
- Li, S., Wang, D.-Z., Wang, Z., Richardson, J. A. and Olson, E. N. (2003). The serum response factor coactivator myocardin is required for vascular smooth muscle development. *Proc. Natl. Acad. Sci. USA* **100**, 9366–9370.
- Liao, Y., Smyth, G. K. and Shi, W. (2013). The Subread aligner: fast, accurate and scalable read mapping by seed-and-vote. *Nucleic Acids Res.* **41**, e108–e108.
- Lin, Q., Schwarz, J., Bucana, C. and Olson, E. N. (1997). Control of mouse cardiac morphogenesis and myogenesis by transcription factor MEF2C. *Science* **276**, 1404–1407.
- Lund, E., Oldenburg, A. R. and Collas, P. (2014). Enriched domain detector: a program for detection of wide genomic enrichment domains robust against local variations. *Nucleic Acids Res.* **42**, e92.
- Martins, A. H. B., Resende, R. R., Majumder, P., Faria, M., Casarini, D. E., Tárnok, A., Colli, W., Pesquero, J. B. and Ulrich, H. (2005). Neuronal differentiation of P19 embryonal carcinoma cells modulates kinin B2 receptor gene expression and function. *J. Biol. Chem.* **280**, 19576–19586.
- Meuleman, W., Peric-Hupkes, D., Kind, J., Beaudry, J.-B., Pagie, L., Kellis, M., Reinders, M., Wessels, L. and van Steensel, B. (2013). Constitutive nuclear lamina-genome interactions are highly conserved and associated with A/T-rich sequence. *Genome Res.* **23**, 270–280.
- Peric-Hupkes, D., Meuleman, W., Pagie, L., Bruggeman, S. W. M., Solovei, I., Brugman, W., Gräf, S., Flieck, P., Kerkhoven, R. M., van Lohuizen, M. et al. (2010). Molecular maps of the reorganization of genome-nuclear lamina interactions during differentiation. *Mol. Cell* **38**, 603–613.

- Poleshko, A., Shah, P. P., Gupta, M., Babu, A., Morley, M. P., Manderfield, L. J., Ifkovits, J. L., Calderon, D., Aghajanian, H., Sierra-Pagán, J. E. et al. (2017). Genome-nuclear lamina interactions regulate cardiac stem cell lineage restriction. *Cell* **171**, 573-580.e14.
- Ritchie, M. E., Phipson, B., Wu, D., Hu, Y., Law, C. W., Shi, W. and Smyth, G. K. (2015). limma powers differential expression analyses for RNA-sequencing and microarray studies. *Nucleic Acids Res.* **43**, e47-e47.
- Robson, M. I., de Las Heras, J. I., Czapiewski, R., Lê Thành, P., Booth, D. G., Kelly, D. A., Webb, S., Kerr, A. R. W. and Schirmer, E. C. (2016). Tissue-specific gene repositioning by muscle nuclear membrane proteins enhances repression of critical developmental genes during myogenesis. *Mol. Cell* **62**, 834-847.
- Rossant, J. and McBurney, M. W. (1982). The developmental potential of a euploid male teratocarcinoma cell line after blastocyst injection. *J. Embryol. Exp. Morphol.* **70**, 99-112.
- Skerjanc, I. S., Petropoulos, H., Ridgeway, A. G. and Wilton, S. (1998). Myocyte enhancer factor 2C and Nkx2-5 up-regulate each other's expression and initiate cardiomyogenesis in P19 cells. *J. Biol. Chem.* **273**, 34904-34910.
- Therizols, P., Illingworth, R. S., Courilleau, C., Boyle, S., Wood, A. J. and Bickmore, W. A. (2014). Chromatin decondensation is sufficient to alter nuclear organization in embryonic stem cells. *Science* **346**, 1238-1242.
- Towbin, B. D., González-Aguilera, C., Sack, R., Gaidatzis, D., Kalck, V., Meister, P., Askjaer, P. and Gasser, S. M. (2012). Step-wise methylation of histone H3K9 positions heterochromatin at the nuclear periphery. *Cell* **150**, 934-947.
- Ueyama, T., Kasahara, H., Ishiwata, T., Nie, Q. and Izumo, S. (2003). Myocardin expression is regulated by Nkx2.5, and its function is required for cardiomyogenesis. *Mol. Cell. Biol.* **23**, 9222-9232.
- van Steensel, B. and Belmont, A. S. (2017). Lamina-associated domains: links with chromosome architecture, heterochromatin, and gene repression. *Cell* **169**, 780-791.
- Wang, D.-Z., Chang, P. S., Wang, Z., Sutherland, L., Richardson, J. A., Small, E., Krieg, P. A. and Olson, E. N. (2001). Activation of cardiac gene expression by myocardin, a transcriptional cofactor for serum response factor. *Cell* **105**, 851-862.
- Yokochi, T., Poduch, K., Ryba, T., Lu, J., Hiratani, I., Tachibana, M., Shinkai, Y. and Gilbert, D. M. (2009). G9a selectively represses a class of late-replicating genes at the nuclear periphery. *Proc. Natl Acad. Sci. USA* **106**, 19363-19368.

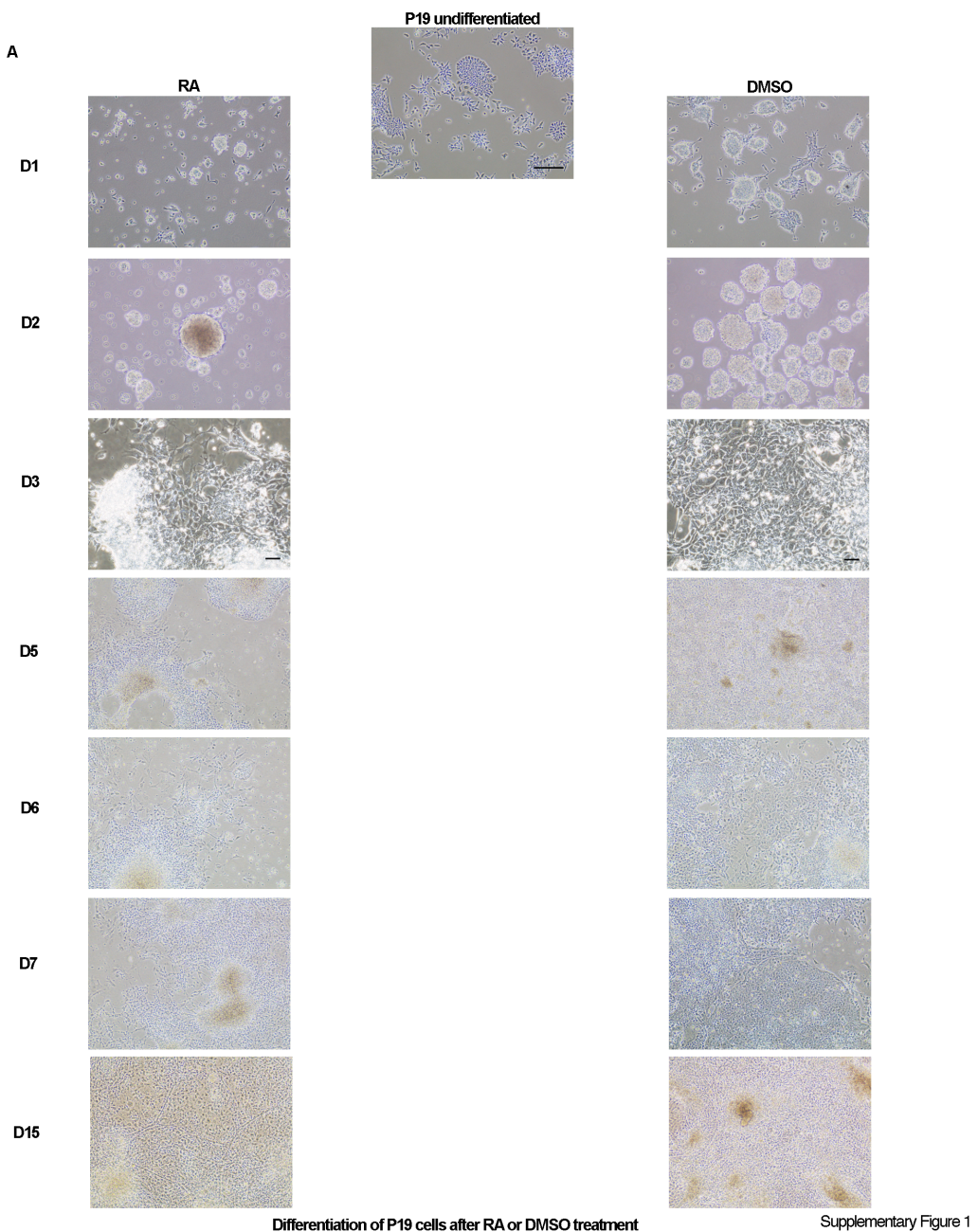
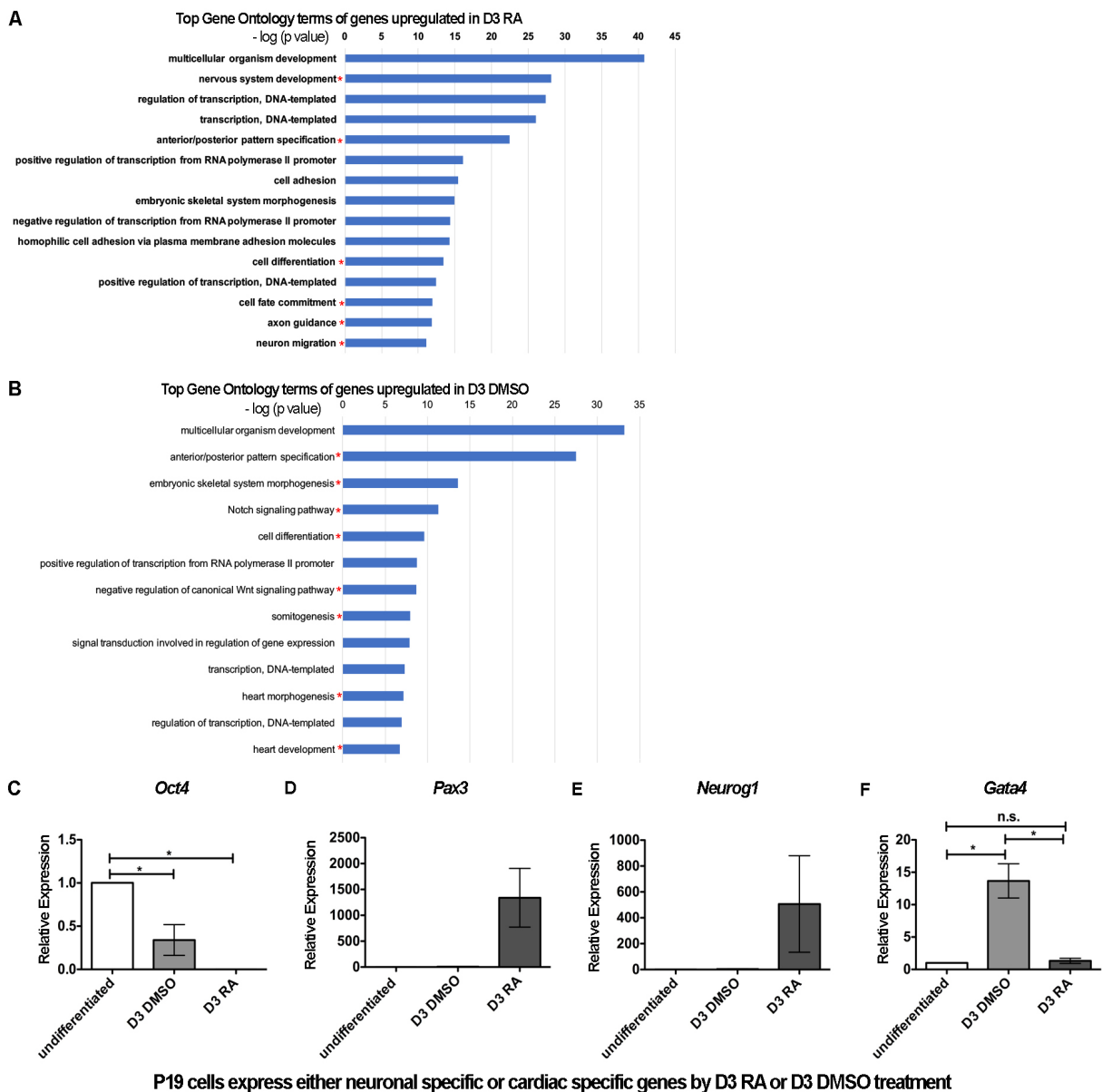


**Fig. S1. Differentiation of P19 cells after RA or DMSO treatment**

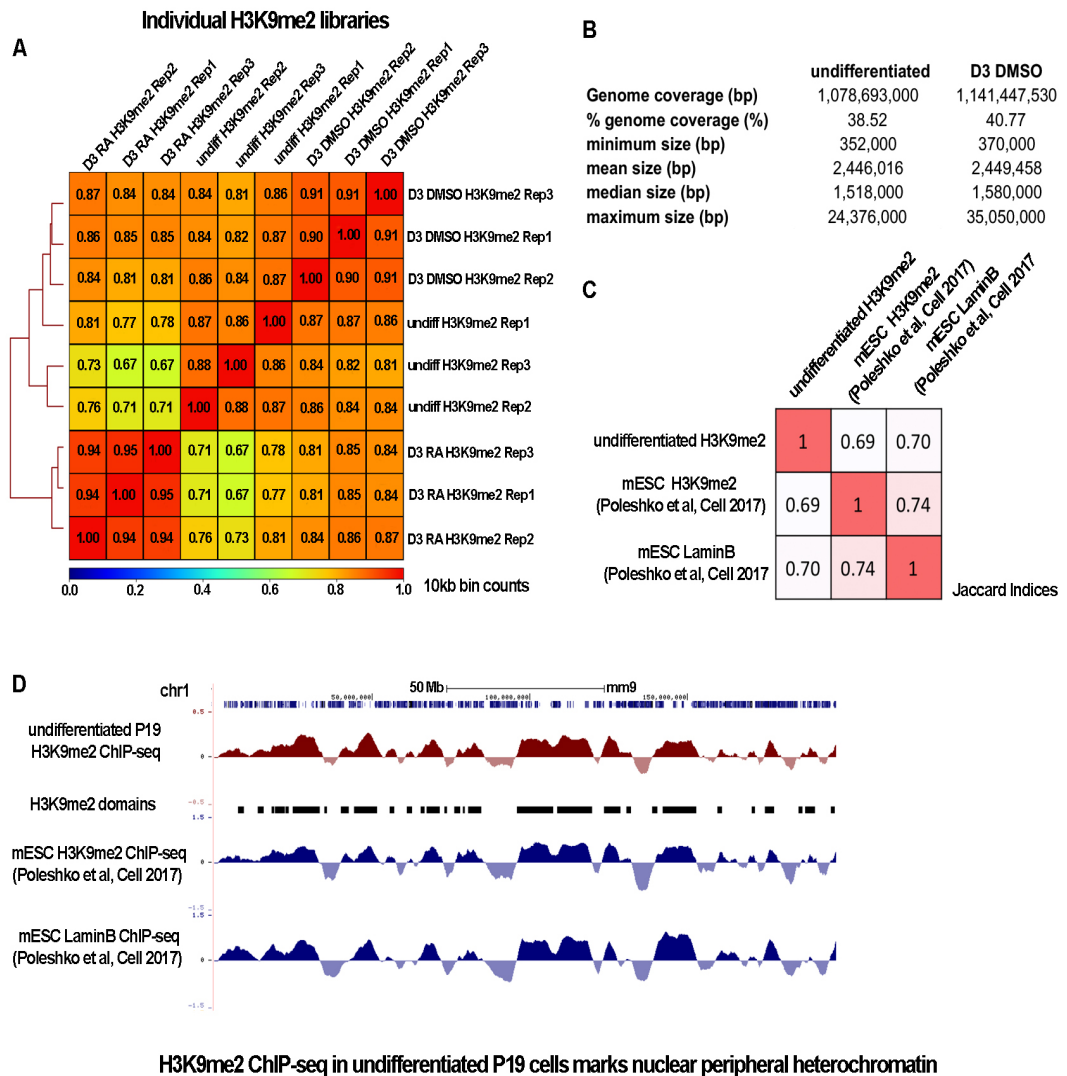
Undifferentiated P19 cells were maintained at low confluence to maintain multipotency. Differentiation of P19 cells were induced via aggregation into embryoid bodies for two days in presence of either 1 $\mu$ M RA or 1% DMSO. Neuronal extensions were evident by day 5 of RA treatment and cells adopted a mesoderm-like morphology by day 6 of DMSO treatment. D: days of treatment. Scale bar 100 $\mu$ m.



Supplementary Figure 2

### Fig. S2. P19 cells express either neuronal-specific or cardiac-specific genes by D3 RA or D3 DMSO treatment

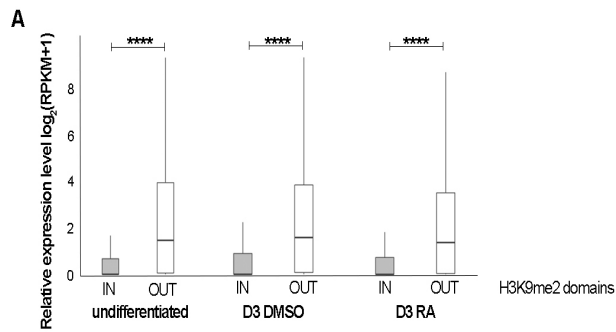
- (A) Top Gene Ontology terms of genes upregulated in D3 RA RNA-seq as compared to undifferentiated.
- (B) Top Gene Ontology terms of genes upregulated in D3 DMSO RNA-seq as compared to undifferentiated.
- (C) Real time RT-qPCR shows significant reduction of Oct4 in D3 DMSO and depletion of Oct4 in D3 RA.
- (D-E) Real time RT-qPCR validates Pax3 and Neurog1 are specifically upregulated in D3 RA.
- (F) Real time RT-qPCR validates that Gata4 is specifically upregulated in D3 DMSO.



Supplementary Figure 3

### Fig. S3. H3K9me2 ChIP-seq in P19 cells marks nuclear peripheral heterochromatin

- Spearman correlation of individual biological replicates of H3K9me2 ChIP-seq using 10kb bin counts in undifferentiated, D3 RA-treated and D3 DMSO-treated P19 cells.
- Genome coverage of H3K9me2 domains defined using merged H3K9me2 ChIP-seq libraries.
- Jaccard Indices of H3K9me2 domains in undifferentiated P19 cells compared to H3K9me2 domains and LaminB domains in mESC (Poleshko et al, Cell 2017).
- Representative ChIP-seq tracks of H3K9me2 ChIP-seq in undifferentiated P19 showing similar domains marked by H3K9me2 ChIP-seq or LaminB ChIP-seq in mESC (Poleshko et al, Cell 2017). Domains indicated by black bars are defined by EDD on H3K9me2 ChIP-seq in undifferentiated P19 cells.



Transcription levels of genes within H3K9me2 domains are lower than genes found outside of H3K9me2 domains

Supplementary Figure 4

**Fig. S4. Transcription levels of genes within H3K9me2 domains are lower than genes found outside of H3K9me2 domains**

(A) Distribution of  $\log_2$  normalized expression levels of genes in H3K9me2 domains and genes outside of H3K9me2 domains in undifferentiated, D3 DMSO and D3 RA P19 cells. Boxplot showing median with maximum and minimum. Mann Whitney U test  $p < 2.2 \times 10^{-16}$

**Table S1. Gene Ontology of upregulated genes in D3 RA-treated**

<b>Term</b>	<b>Count</b>	<b>%</b>	<b>P Value</b>
GO:0007275~multicellular organism development	169	14.54388985	1.66E-41
<b>GO:0007399~nervous system development</b>	83	7.142857143	7.02E-29
GO:0006355~regulation of transcription, DNA-templated	242	20.82616179	4.04E-28
GO:0006351~transcription, DNA-templated	210	18.07228916	9.15E-27
<b>GO:0009952~anterior/posterior pattern specification</b>	41	3.528399312	3.57E-23
GO:0045944~positive regulation of transcription from RNA polymerase II promoter	118	10.15490534	8.23E-17
GO:0007155~cell adhesion	74	6.368330465	3.99E-16
GO:0048704~embryonic skeletal system morphogenesis	24	2.065404475	1.25E-15
GO:0000122~negative regulation of transcription from RNA polymerase II promoter	93	8.003442341	4.53E-15
GO:0007156~homophilic cell adhesion via plasma membrane adhesion molecules	39	3.356282272	5.25E-15
<b>GO:0030154~cell differentiation</b>	95	8.17555938	3.86E-14
GO:0045893~positive regulation of transcription, DNA-templated	76	6.540447504	3.72E-13
<b>GO:0045165~cell fate commitment</b>	24	2.065404475	1.08E-12
<b>GO:0007411~axon guidance</b>	34	2.925989673	1.52E-12
<b>GO:0001764~neuron migration</b>	30	2.581755594	8.21E-12
GO:0051216~cartilage development	24	2.065404475	2.22E-11
GO:0045665~negative regulation of neuron differentiation	23	1.979345955	3.05E-11
GO:0042472~inner ear morphogenesis	22	1.893287435	7.31E-11
GO:0010001~glial cell differentiation	13	1.118760757	8.42E-11
GO:0001525~angiogenesis	40	3.442340792	3.04E-10
GO:0008285~negative regulation of cell proliferation	51	4.388984509	3.52E-09
GO:0001656~metanephros development	15	1.290877797	3.57E-09
<b>GO:0030182~neuron differentiation</b>	26	2.237521515	1.02E-08
<b>GO:0048663~neuron fate commitment</b>	13	1.118760757	3.76E-08
<b>GO:0021527~spinal cord association neuron differentiation</b>	9	0.774526678	6.02E-08
GO:0045892~negative regulation of transcription, DNA-templated	63	5.421686747	9.34E-08
GO:0001657~ureteric bud development	15	1.290877797	1.08E-07

GO:0007219~Notch signaling pathway	24	2.065404475	1.45E-07
GO:0030501~positive regulation of bone mineralization	13	1.118760757	2.41E-07
GO:0048706~embryonic skeletal system development	14	1.204819277	2.61E-07
GO:0007507~heart development	36	3.098106713	3.87E-07
GO:0001503~ossification	20	1.721170396	5.40E-07
<b>GO:0007409~axonogenesis</b>	21	1.807228916	7.17E-07
GO:0001822~kidney development	23	1.979345955	1.19E-06
GO:0008284~positive regulation of cell proliferation	57	4.905335628	1.24E-06
<b>GO:0010842~retina layer formation</b>	10	0.860585198	1.30E-06
GO:0048839~inner ear development	16	1.376936317	1.34E-06
<b>GO:0051965~positive regulation of synapse assembly</b>	16	1.376936317	2.96E-06
GO:0030335~positive regulation of cell migration	29	2.495697074	3.19E-06
<b>GO:0007417~central nervous system development</b>	18	1.549053356	3.54E-06
GO:0045446~endothelial cell differentiation	7	0.602409639	3.76E-06
<b>GO:0071300~cellular response to retinoic acid</b>	15	1.290877797	5.91E-06
<b>GO:0022008~neurogenesis</b>	15	1.290877797	5.91E-06
GO:0001755~neural crest cell migration	13	1.118760757	6.68E-06
<b>GO:0045666~positive regulation of neuron differentiation</b>	19	1.635111876	6.89E-06
GO:0035881~amacrine cell differentiation	6	0.516351119	7.85E-06
GO:0007626~locomotory behavior	19	1.635111876	1.36E-05
GO:0009887~organ morphogenesis	19	1.635111876	1.55E-05
GO:0045746~negative regulation of Notch signaling pathway	10	0.860585198	2.18E-05
GO:0001945~lymph vessel development	7	0.602409639	2.68E-05

**Table S2. Gene Ontology of upregulated genes in D3 DMSO-treated**

<b>Term</b>	<b>Count</b>	<b>%</b>	<b>P Value</b>
GO:0007275~multicellular organism development	115	17.5304878	6.79E-34
<b>GO:0009952~anterior/posterior pattern specification</b>	38	5.792682927	3.24E-28
<b>GO:0048704~embryonic skeletal system morphogenesis</b>	19	2.896341463	2.77E-14
<b>GO:0007219~Notch signaling pathway</b>	24	3.658536585	5.36E-12
GO:0030154~cell differentiation	60	9.146341463	2.44E-10
GO:0045944~positive regulation of transcription from RNA polymerase II promoter	68	10.36585366	1.86E-09
<b>GO:0090090~negative regulation of canonical Wnt signaling pathway</b>	19	2.896341463	2.24E-09
<b>GO:0001756~somitogenesis</b>	14	2.134146341	1.22E-08
GO:0023019~signal transduction involved in regulation of gene expression	10	1.524390244	1.41E-08
GO:0006351~transcription, DNA-templated	101	15.39634146	5.51E-08
<b>GO:0003007~heart morphogenesis</b>	14	2.134146341	6.76E-08
GO:0006355~regulation of transcription, DNA-templated	115	17.5304878	1.24E-07
<b>GO:0007507~heart development</b>	27	4.115853659	1.83E-07
GO:0007411~axon guidance	20	3.048780488	1.91E-07
GO:0001706~endoderm formation	8	1.219512195	2.42E-07
GO:0030335~positive regulation of cell migration	23	3.506097561	3.81E-07
<b>GO:0048706~embryonic skeletal system development</b>	11	1.676829268	7.43E-07
GO:0008284~positive regulation of cell proliferation	40	6.097560976	1.09E-06
GO:0051216~cartilage development	14	2.134146341	1.38E-06
GO:0009887~organ morphogenesis	16	2.43902439	1.39E-06
GO:0009653~anatomical structure morphogenesis	8	1.219512195	1.47E-06

GO:0000122~negative regulation of transcription from RNA polymerase II promoter	48	7.317073171	1.93E-06
<b>GO:0060070~canonical Wnt signaling pathway</b>	14	2.134146341	3.56E-06
GO:0007368~determination of left/right symmetry	13	1.981707317	7.24E-06
GO:0030878~thyroid gland development	8	1.219512195	1.06E-05
GO:0042472~inner ear morphogenesis	12	1.829268293	1.29E-05
GO:0001755~neural crest cell migration	10	1.524390244	1.72E-05
GO:0030879~mammary gland development	9	1.37195122	1.78E-05
GO:0008045~motor neuron axon guidance	8	1.219512195	1.81E-05
<b>GO:0001947~heart looping</b>	11	1.676829268	1.95E-05

**Table S3. Sequencing reads for ChIP-seq**

Sample	Reads (uniquely mapped and deduplicated)
D0-H3-Rep1	43086974
D0-H3-Rep2	30729179
D0-H3-Rep3	23839747
D0-H3K9me2-Rep1	37789704
D0-H3K9me2-Rep2	33939137
D0-H3K9me2-Rep3	35347402
D3DMSO-H3-Rep1	35323181
D3DMSO-H3-Rep2	52573539
D3DMSO-H3-Rep3	28546474
D3DMSO-H3K9me2-Rep1	51219242
D3DMSO-H3K9me2-Rep2	41901201
D3DMSO-H3K9me2-Rep3	37456034
D3RA-H3-Rep1	38493423
D3RA-H3-Rep2	32611274
D3RA-H3-Rep3	31765433
D3RA-H3K9me2-Rep1	40576896
D3RA-H3K9me2-Rep2	36173487
D3RA-H3K9me2-Rep3	37238213
<b>Average</b>	37145030

**Table S4. Sequence of primers used**

Name	Primer Sequence (5' -> 3')
gapdh qPCR Fwd	gggttcctataaatacggactgc
gapdh qPCR Rev	ccattttgtctacgggacga
Pou5f1 qPCR Fwd	accctgggcgttcttt
Pou5f1 qPCR Rev	gttgtcggcttcctccac
Pax3 qPCR Fwd	gcgagaaaaaggctaaacaca
Pax3 qPCR Rev	cggagccatctgactg
Neurogenin1 qPCR Fwd	gacctgtccagcttcac
Neurogenin1 qPCR Rev	tggaggctagggctgttag
Gata4 qPCR Fwd	tctaagacgccagcaggc
Gata4 qPCR Rev	tgctgctgctgtagtgg
Myocd qPCR Fwd	ccccagacatcaaattccact
Myocd qPCR Rev	ctgagccaggagtgagatcc
Mef2c qPCR Fwd	atgggcggagatctgaca
Mef2c qPCR Rev	ttcttgttcaggattaccaggt

**Table S5. Genes within H3K9me2 domains specifically lost in D3 RA**

<b>SYMBOL</b>	<b>ENSEMBL</b>	<b>BIOTYPE</b>	<b>Gene Location</b>
1700111E14Rik	ENSMUSG00000029837	protein_coding	chr6:36887048-36935777
1700112E06Rik	ENSMUSG00000063458	protein_coding	chr14:22838934-23875307
2810007J24Rik	ENSMUSG00000030378	protein_coding	chr7:14996036-15032118
2810055G20Rik	ENSMUSG00000052450	protein_coding	chr16:77500751-77598776
2810055G20Rik	ENSMUSG00000090386	protein_coding	chr16:77329504-77598689
4930533L02Rik	ENSMUSG00000051614	protein_coding	chr7:132461873-132463032
4930544G11Rik	ENSMUSG00000036463	protein_coding	chr6:65902565-65904006
9130008F23Rik	ENSMUSG00000054951	protein_coding	chr17:41012431-41017507
9230109A22Rik	ENSMUSG00000051237	protein_coding	chr15:25067285-25078914
A130050O07Rik	ENSMUSG00000051480	protein_coding	chr1:139824747-139826850
A930038C07Rik	ENSMUSG00000049001	protein_coding	chr6:65621584-65656924
Aard	ENSMUSG00000068522	protein_coding	chr15:51871653-51877267
Abca1	ENSMUSG00000015243	protein_coding	chr4:53043659-53172767
Aimp1	ENSMUSG00000028029	protein_coding	chr3:132323462-132346843
Alg10b	ENSMUSG00000075470	protein_coding	chr15:90054742-90060985
<b>App</b>	ENSMUSG00000022892	protein_coding	chr16:84954685-85173952
Atp11c	ENSMUSG00000062949	protein_coding	chrX:57476467-57845873
Atp6v1g3	ENSMUSG00000026394	protein_coding	chr1:140170315-140186037
Atpbd4	ENSMUSG00000057147	protein_coding	chr2:114342152-114480700
AW146154	ENSMUSG00000074166	protein_coding	chr7:48734250-48755260
B630005N14Rik	ENSMUSG00000042742	protein_coding	chr6:13575677-13627966
BC003331	ENSMUSG0000006010	protein_coding	chr1:152208435-152240210
BC052040	ENSMUSG00000040282	protein_coding	chr2:115407452-115604504
Btg1	ENSMUSG00000036478	protein_coding	chr10:96079635-96085447
Btg3	ENSMUSG00000022863	protein_coding	chr16:78360105-78377437
C130060K24Rik	ENSMUSG00000029917	protein_coding	chr6:65331099-65408144
C1d	ENSMUSG0000000581	protein_coding	chr11:17157582-17169179
C1qtnf7	ENSMUSG00000061535	protein_coding	chr5:43906808-44010056
Camk2d	ENSMUSG00000053819	protein_coding	chr3:126299220-126547972
<b>Camk4</b>	ENSMUSG00000038128	protein_coding	chr18:33098695-33355421
Capza2	ENSMUSG00000015733	protein_coding	chr6:17586234-17616972
Cav1	ENSMUSG00000007655	protein_coding	chr6:17256335-17291452
Cav2	ENSMUSG00000000058	protein_coding	chr6:17231185-17239115
Ccnh	ENSMUSG00000021548	protein_coding	chr13:85329013-85363074
Cenpq	ENSMUSG00000023919	protein_coding	chr17:41060000-41071996
Cnrip1	ENSMUSG00000044629	protein_coding	chr11:16951589-16979374
Cpeb2	ENSMUSG00000039782	protein_coding	chr5:43624702-43680963
Cpne8	ENSMUSG00000052560	protein_coding	chr15:90317913-90509863
Csl	ENSMUSG00000046934	protein_coding	chr10:99220339-99222292
Cxadr	ENSMUSG00000022865	protein_coding	chr16:78301741-78360030
Cyclc1	ENSMUSG00000073001	protein_coding	chrX:108305797-108319213
<b>D0H4S114</b>	ENSMUSG00000042834	protein_coding	chr18:33596673-33623683
D16Ert472e	ENSMUSG00000022864	protein_coding	chr16:78544257-78576902
D630013G24Rik	ENSMUSG00000040969	protein_coding	chr3:132775242-132897913
Dbx2	ENSMUSG00000045608	protein_coding	chr15:95453994-95486391
<b>Dpysl3</b>	ENSMUSG00000024501	protein_coding	chr18:43480633-43597940
Dsg1a	ENSMUSG00000069441	protein_coding	chr18:20469312-20501851
Dsg1b	ENSMUSG00000061928	protein_coding	chr18:20535230-20568697
Dsg3	ENSMUSG00000056632	protein_coding	chr18:20668805-20705360
Dsg4	ENSMUSG0000001804	protein_coding	chr18:20594676-20630322
Egfem1	ENSMUSG00000063600	protein_coding	chr3:28980945-29590126
Egfr	ENSMUSG00000020122	protein_coding	chr11:16652206-16818161
Eif3h	ENSMUSG00000022312	protein_coding	chr15:51618104-51697027
Eny2	ENSMUSG00000022338	protein_coding	chr15:44259657-44269231
F9	ENSMUSG00000031138	protein_coding	chrX:57252641-57283936

Fam155a	ENSMUSG00000079157	protein_coding	chr8:9207238-9771018
Fam179b	ENSMUSG00000035614	protein_coding	chr12:66066729-66123560
Fam198b	ENSMUSG00000027955	protein_coding	chr3:79688455-79750202
Fam59a	ENSMUSG00000042680	protein_coding	chr18:21285702-21458639
Fancm	ENSMUSG00000055884	protein_coding	chr12:66176593-66233045
Fbxo48	ENSMUSG00000044966	protein_coding	chr11:16851378-16854775
Fkbp3	ENSMUSG00000020949	protein_coding	chr12:66163423-66174931
Fpr-rs3	ENSMUSG00000060701	protein_coding	chr17:20760810-20761841
Fpr-rs6	ENSMUSG00000071275	protein_coding	chr17:20319042-20320061
Fpr-rs7	ENSMUSG00000071276	protein_coding	chr17:20250174-20251190
<b>Gap43</b>	ENSMUSG00000047261	protein_coding	chr16:42248555-42340764
Gk2	ENSMUSG00000050553	protein_coding	chr5:97884180-97886027
Glyatl3	ENSMUSG00000091043	protein_coding	chr17:41041690-41051299
Gm10287	ENSMUSG00000070342	protein_coding	chr3:148884657-148888709
Gm10291	ENSMUSG00000070443	protein_coding	chr3:78721130-78722380
Gm10549	ENSMUSG00000073610	protein_coding	chr18:33623817-33632102
Gm11146	ENSMUSG00000079546	protein_coding	chr16:77588823-77602339
Gm1527	ENSMUSG00000074655	protein_coding	chr3:28791539-28825646
Gm17333	ENSMUSG00000091193	protein_coding	chr16:77846938-77853265
Gm17350	ENSMUSG00000091977	protein_coding	chr8:130870807-130870971
Gm17618	ENSMUSG00000091767	protein_coding	chr13:84544444-84545077
Gm17664	ENSMUSG00000091489	protein_coding	chr11:16662047-16662263
Gm4066	ENSMUSG00000091518	protein_coding	chr13:85164700-85164939
Gm4301	ENSMUSG00000091918	protein_coding	chr10:99798310-99799225
Gm4302	ENSMUSG00000091101	protein_coding	chr10:99803490-99804374
Gm4303	ENSMUSG00000090421	protein_coding	chr10:99808624-99809493
Gm4305	ENSMUSG00000091715	protein_coding	chr10:99813745-99814614
Gm4307	ENSMUSG00000091170	protein_coding	chr10:99823990-99824859
Gm4308	ENSMUSG00000091145	protein_coding	chr10:99829133-99830048
Gm4312	ENSMUSG00000091915	protein_coding	chr10:99844279-99845194
Gm4781	ENSMUSG00000090987	protein_coding	chr10:99858921-99859706
Gm5145	ENSMUSG00000071273	protein_coding	chr17:20707326-20708162
Gm527	ENSMUSG00000047227	protein_coding	chr12:66018898-66025578
Gm5670	ENSMUSG00000059827	protein_coding	chr14:23377304-23377675
Gm6871	ENSMUSG00000090744	protein_coding	chr7:48801044-48829032
Gm7073	ENSMUSG00000079583	protein_coding	chrX:57689227-57705652
Gm7854	ENSMUSG00000085720	protein_coding	chr5:43626241-43626591
Gm8181	ENSMUSG00000048188	protein_coding	chr18:43330759-43332247
Gm8701	ENSMUSG00000091739	protein_coding	chr10:99788062-99794069
Gm8759	ENSMUSG00000067870	protein_coding	chr15:90594677-90595092
Gm9781	ENSMUSG00000043424	protein_coding	chr18:43635074-43637450
Gm9843	ENSMUSG00000050299	protein_coding	chr16:76403454-76403957
Gm9912	ENSMUSG00000053583	protein_coding	chr3:148848115-148848459
Gm9954	ENSMUSG00000054714	protein_coding	chr5:64041189-64041503
Gpr125	ENSMUSG00000029090	protein_coding	chr5:50351190-50450235
Gpr158	ENSMUSG00000045967	protein_coding	chr2:21289169-21752174
Gstcd	ENSMUSG00000028018	protein_coding	chr3:132644717-132754997
Has2	ENSMUSG00000022367	protein_coding	chr15:56497182-56526094
Hhip	ENSMUSG00000064325	protein_coding	chr8:82490014-82581905
Hmcn1	ENSMUSG00000066842	protein_coding	chr1:152410657-152840565
Hnmt	ENSMUSG00000026986	protein_coding	chr2:23858430-23904914
Ints12	ENSMUSG00000028016	protein_coding	chr3:132754804-132773952
Jakmip2	ENSMUSG00000024502	protein_coding	chr18:43691062-43847427
Kif21a	ENSMUSG00000022629	protein_coding	chr15:90763707-90880382
Kitl	ENSMUSG00000019966	protein_coding	chr10:99478264-99563047
Klhl14	ENSMUSG00000042514	protein_coding	chr18:21708878-21813219
Klhl28	ENSMUSG00000020948	protein_coding	chr12:66043427-66066523
Lphn2	ENSMUSG00000028184	protein_coding	chr3:148478550-148652280

Lrrc69	ENSMUSG00000023151	protein_coding	chr4:14550767-14723207
Mad2l1	ENSMUSG00000029910	protein_coding	chr6:66485384-66491027
<b>Mcf2</b>	ENSMUSG00000031139	protein_coding	chrX:57309131-57432266
<b>Mecom</b>	ENSMUSG00000027684	protein_coding	chr3:29850221-30446930
<b>Mef2c</b>	ENSMUSG00000005583	protein_coding	chr13:83643033-83806684
<b>Met</b>	ENSMUSG00000009376	protein_coding	chr6:17413800-17523980
Mis18bp1	ENSMUSG00000047534	protein_coding	chr12:66233721-66273591
Mut	ENSMUSG00000023921	protein_coding	chr17:41071656-41098582
Naa11	ENSMUSG00000046000	protein_coding	chr5:97811243-97821349
Nell2	ENSMUSG00000022454	protein_coding	chr15:94905661-95359137
Ngly1	ENSMUSG00000021785	protein_coding	chr14:17081794-17144440
Nhs	ENSMUSG00000059493	protein_coding	chrX:158271228-158597662
Nipsnap3b	ENSMUSG00000015247	protein_coding	chr4:53024752-53034932
Npnt	ENSMUSG00000040998	protein_coding	chr3:132544709-132613255
Nrip1	ENSMUSG00000048490	protein_coding	chr16:76287645-76374072
<b>Nrp1</b>	ENSMUSG00000025810	protein_coding	chr8:130882973-131029362
Olfr135	ENSMUSG00000057801	protein_coding	chr17:38345114-38346192
Olfr137	ENSMUSG00000054940	protein_coding	chr17:38441464-38442405
Olfr138	ENSMUSG00000057443	protein_coding	chr17:38398012-38412656
Olfr1459	ENSMUSG00000057503	protein_coding	chr19:13220133-13221233
Olfr1461	ENSMUSG00000045883	protein_coding	chr19:13239506-13240444
Olfr1462	ENSMUSG00000058800	protein_coding	chr19:13265159-13266082
Olfr1463	ENSMUSG00000052277	protein_coding	chr19:13308742-13309674
Olfr1465	ENSMUSG00000062199	protein_coding	chr19:13387850-13388773
Olfr1466	ENSMUSG00000062936	protein_coding	chr19:13416250-13417182
Olfr1467	ENSMUSG00000049015	protein_coding	chr19:13439120-13440046
Olfr1469	ENSMUSG00000063777	protein_coding	chr19:13485061-13485990
Olfr1471	ENSMUSG00000056670	protein_coding	chr19:13519504-13520448
Olfr1472	ENSMUSG00000058949	protein_coding	chr19:13528061-13529005
Olfr1474	ENSMUSG00000071630	protein_coding	chr19:13545462-13546406
Olfr1475	ENSMUSG00000062195	protein_coding	chr19:13553742-13554686
Olfr1477	ENSMUSG00000071629	protein_coding	chr19:13575036-13577782
Olfr1480	ENSMUSG00000063485	protein_coding	chr19:13604165-13605112
Olfr1484	ENSMUSG00000057213	protein_coding	chr19:13659796-13660743
Olfr1487	ENSMUSG00000057950	protein_coding	chr19:13693654-13694601
Olfr1489	ENSMUSG00000045678	protein_coding	chr19:13707603-13708544
Olfr1490	ENSMUSG00000061387	protein_coding	chr19:13728936-13729886
Olfr1491	ENSMUSG00000051156	protein_coding	chr19:13779319-13780278
Olfr1494	ENSMUSG00000050865	protein_coding	chr19:13823598-13824545
Olfr1495	ENSMUSG00000047207	protein_coding	chr19:13842797-13843885
Olfr1496	ENSMUSG00000048356	protein_coding	chr19:13855038-13856104
Olfr1497	ENSMUSG00000044040	protein_coding	chr19:13869155-13870099
Olfr1499	ENSMUSG00000045395	protein_coding	chr19:13889097-13890148
Olfr1500	ENSMUSG00000054526	protein_coding	chr19:13901925-13902949
Olfr1501	ENSMUSG00000057270	protein_coding	chr19:13912714-13913661
Olfr1502	ENSMUSG00000056858	protein_coding	chr19:13936285-13937235
Olfr1504	ENSMUSG00000059105	protein_coding	chr19:13961711-13962795
Olfr1505	ENSMUSG00000062314	protein_coding	chr19:13993432-13994534
Olfr711	ENSMUSG00000045013	protein_coding	chr7:114114882-114118965
Otud6b	ENSMUSG00000040550	protein_coding	chr4:14736645-14753734
Oxsm	ENSMUSG00000021786	protein_coding	chr14:17071170-17082322
Pard3b	ENSMUSG00000052062	protein_coding	chr1:61685398-62688858
Pdc	ENSMUSG0000006007	protein_coding	chr1:152166547-152181035
<b>Pcl1</b>	ENSMUSG00000038349	protein_coding	chr1:55463232-55808646
Plek	ENSMUSG00000020120	protein_coding	chr11:16871209-16952384
Pno1	ENSMUSG00000020116	protein_coding	chr11:17103201-17111571
Ppa2	ENSMUSG00000028013	protein_coding	chr3:132973074-133041199
Ppp3r1	ENSMUSG00000033953	protein_coding	chr11:17059266-17100378

Prdm5	ENSMUSG00000029913	protein_coding	chr6:65728982-65886367
Prg4	ENSMUSG00000006014	protein_coding	chr1:152296542-152313295
Prpf39	ENSMUSG00000035597	protein_coding	chr12:66137320-66164373
<b>Ptn</b>	ENSMUSG00000029838	protein_coding	chr6:36665663-36761361
Ptprc	ENSMUSG00000026395	protein_coding	chr1:139959438-140071882
Rad21	ENSMUSG00000022314	protein_coding	chr15:51794151-51823306
<b>Rai2</b>	ENSMUSG00000043518	protein_coding	chrX:158155001-158217428
<b>Rarb</b>	ENSMUSG00000017491	protein_coding	chr14:17263356-17651381
Rasa1	ENSMUSG00000021549	protein_coding	chr13:85354304-85429091
Rbpsuh-rs3	ENSMUSG00000079575	protein_coding	chr6:46479350-46480921
Rhag	ENSMUSG00000023926	protein_coding	chr17:40948075-40977703
Runx1t1	ENSMUSG0000006586	protein_coding	chr4:13670583-13820796
Sec61g	ENSMUSG00000078974	protein_coding	chr11:16400533-16408487
Slc26a7	ENSMUSG00000040569	protein_coding	chr4:14429577-14548952
<b>Sox3</b>	ENSMUSG00000045179	protein_coding	chrX:58144545-58146605
Spopl	ENSMUSG00000026771	protein_coding	chr2:23361740-23427626
<b>St7</b>	ENSMUSG00000029534	protein_coding	chr6:17642933-17893025
Stard4	ENSMUSG00000024378	protein_coding	chr18:33359009-33373516
Stk32a	ENSMUSG00000039954	protein_coding	chr18:43367351-43477135
<b>Sv2b</b>	ENSMUSG00000053025	protein_coding	chr7:82259783-82454148
<b>Syt10</b>	ENSMUSG00000063260	protein_coding	chr15:89612824-89672291
Tbck	ENSMUSG00000028030	protein_coding	chr3:132347108-132501470
Tbpl2	ENSMUSG00000061809	protein_coding	chr2:23927241-23952115
<b>Tcf4</b>	ENSMUSG00000053477	protein_coding	chr18:69503800-69847621
Tes	ENSMUSG00000029552	protein_coding	chr6:17015149-17055828
<b>Tet2</b>	ENSMUSG00000040943	protein_coding	chr3:133126643-133207354
Tfec	ENSMUSG00000029553	protein_coding	chr6:16783381-16848441
Tle4	ENSMUSG00000024642	protein_coding	chr19:14522562-14672473
Tmem161b	ENSMUSG00000035762	protein_coding	chr13:84361901-84435571
Tmem168	ENSMUSG00000029569	protein_coding	chr6:13530687-13558100
Tmem55a	ENSMUSG00000028221	protein_coding	chr4:14791223-14842323
Tnip3	ENSMUSG00000044162	protein_coding	chr6:65540392-65584034
<b>Top2b</b>	ENSMUSG00000017485	protein_coding	chr14:17197693-17263301
Tpr	ENSMUSG00000006005	protein_coding	chr1:152239968-152297065
Trib2	ENSMUSG00000020601	protein_coding	chr12:15798533-15823683
Usp25	ENSMUSG00000022867	protein_coding	chr16:77014314-77117024
Utp23	ENSMUSG00000022313	protein_coding	chr15:51708975-51716160
Vmn1r224	ENSMUSG00000091151	protein_coding	chr17:20556127-20557023
Vmn1r225	ENSMUSG00000043537	protein_coding	chr17:20639263-20640159
Vmn1r226	ENSMUSG00000042848	protein_coding	chr17:20824472-20825368
Vmn1r228	ENSMUSG00000060245	protein_coding	chr17:20913026-20914465
Vmn1r229	ENSMUSG00000061150	protein_coding	chr17:20951459-20952379
Vmn1r230	ENSMUSG00000045417	protein_coding	chr17:20983515-20984465
Vmn1r231	ENSMUSG00000050933	protein_coding	chr17:21026155-21027684
Vmn1r232	ENSMUSG00000062165	protein_coding	chr17:21050169-21051327
Vmn1r32	ENSMUSG00000062905	protein_coding	chr6:66502177-66509702
Vmn1r33	ENSMUSG00000059375	protein_coding	chr6:66561442-66566056
Vmn1r34	ENSMUSG00000091012	protein_coding	chr6:66586817-66587746
Vmn1r35	ENSMUSG00000060699	protein_coding	chr6:66628788-66629678
Vmn1r37	ENSMUSG00000057612	protein_coding	chr6:66681386-66682294
Vmn2r100	ENSMUSG00000091859	protein_coding	chr17:19641775-19669024
Vmn2r101	ENSMUSG00000090680	protein_coding	chr17:19714195-19749281
Vmn2r102	ENSMUSG00000090884	protein_coding	chr17:19797363-19831712
Vmn2r103	ENSMUSG00000091771	protein_coding	chr17:19910327-19949500
Vmn2r104	ENSMUSG00000090315	protein_coding	chr17:20166389-20185169
Vmn2r105	ENSMUSG00000091670	protein_coding	chr17:20345194-20371836
Vmn2r106	ENSMUSG00000091656	protein_coding	chr17:20404511-20422394
Vmn2r107	ENSMUSG00000056910	protein_coding	chr17:20482389-20512736

Vmn2r108	ENSMUSG00000091805	protein_coding	chr17:20599337-20618200
Vmn2r109	ENSMUSG00000090572	protein_coding	chr17:20677481-20701720
Vmn2r110	ENSMUSG00000091259	protein_coding	chr17:20710793-20733223
Vmn2r97	ENSMUSG00000091491	protein_coding	chr17:19051286-19085035
Vmn2r98	ENSMUSG00000090851	protein_coding	chr17:19190457-19218275
Vmn2r99	ENSMUSG00000090304	protein_coding	chr17:19499099-19531554
Wdr92	ENSMUSG00000078970	protein_coding	chr11:17082110-17135203
Zbtb20	ENSMUSG00000022708	protein_coding	chr16:42875994-43642715

**Table S6. Genes within H3K9me2 domains specifically lost in D3 DMSO**

SYMBOL	ENSEMBL	BIOTYPE	Gene Location
1700012A03Rik	ENSMUSG00000029766	protein_coding	chr6:32000246-32008921
1700056E22Rik	ENSMUSG00000044854	protein_coding	chr1:185856911-185857453
1700061I17Rik	ENSMUSG00000028009	protein_coding	chr3:116763440-116780683
1700086D15Rik	ENSMUSG00000020548	protein_coding	chr11:64965412-64973393
1700108M19Rik	ENSMUSG00000020545	protein_coding	chr12:36934932-36979985
1810046K07Rik	ENSMUSG00000036027	protein_coding	chr9:51097791-51137022
2010007H06Rik	ENSMUSG00000044694	protein_coding	chr9:51088400-51089025
2010109K11Rik	ENSMUSG00000090946	protein_coding	chr12:33063569-33067808
2610303G11Rik	ENSMUSG00000046995	protein_coding	chr9:98086946-98087571
2810407A14Rik	ENSMUSG00000055972	protein_coding	chr16:87784320-87793846
3110018I06Rik	ENSMUSG00000060375	protein_coding	chr12:108726842-108727846
4833423E24Rik	ENSMUSG00000075217	protein_coding	chr2:85323751-85359181
4930455H04Rik	ENSMUSG00000080907	protein_coding	chr3:116671185-116687324
4931431F19Rik	ENSMUSG00000055643	protein_coding	chr7:111276427-111278337
5031434C07Rik	ENSMUSG00000044574	protein_coding	chr6:112235851-112238831
A330050F15Rik	ENSMUSG00000091636	protein_coding	chr17:69788666-69838573
A530021J07Rik	ENSMUSG00000053528	protein_coding	chr7:90297154-90304432
A630010A05Rik	ENSMUSG00000075395	protein_coding	chr16:14562409-14621393
Abpe	ENSMUSG00000036521	protein_coding	chr7:32087780-32089996
Abph	ENSMUSG00000062556	protein_coding	chr7:32075539-32076835
<b>Adamts1</b>	ENSMUSG00000022893	protein_coding	chr16:85794072-85803358
Adamts18	ENSMUSG00000053399	protein_coding	chr8:116221026-116372641
<b>Adcy2</b>	ENSMUSG00000021536	protein_coding	chr13:68758920-69138419
Ag2	ENSMUSG00000020581	protein_coding	chr12:36719494-36730674
Ag3	ENSMUSG00000036231	protein_coding	chr12:36652207-36676323
Alk	ENSMUSG00000055471	protein_coding	chr17:72218782-72953049
Ankmy2	ENSMUSG00000036188	protein_coding	chr12:36883711-36923878
Ankrd50	ENSMUSG00000044864	protein_coding	chr3:38348183-38383766

Ano2	ENSMUSG00000038115	protein_coding	chr6:125640437-125990144
Ano3	ENSMUSG00000074968	protein_coding	chr2:110495358-110791080
Aqp4	ENSMUSG00000024411	protein_coding	chr18:15547903-15562193
Arhgap20	ENSMUSG00000053199	protein_coding	chr9:51573442-51661961
<b>Arhgap26</b>	ENSMUSG00000036452	protein_coding	chr18:38761188-39535938
Arrdc4	ENSMUSG00000042659	protein_coding	chr7:75881931-75894127
Atoh1	ENSMUSG00000073043	protein_coding	chr6:64679140-64681227
Bach1	ENSMUSG00000025612	protein_coding	chr16:87699190-87733591
Bbox1	ENSMUSG00000041660	protein_coding	chr2:110102854-110154717
BC053393	ENSMUSG00000046974	protein_coding	chr11:46385038-46402734
<b>Bdnf</b>	ENSMUSG00000048482	protein_coding	chr2:109514857-109567164
Bzw2	ENSMUSG00000020547	protein_coding	chr12:36818433-36883412
C030034I22Rik	ENSMUSG00000073374	protein_coding	chr17:69766801-69768271
C330027C09Rik	ENSMUSG00000033031	protein_coding	chr16:48994298-49019822
C8a	ENSMUSG00000035031	protein_coding	chr4:104488284-104549003
C8b	ENSMUSG00000029656	protein_coding	chr4:104438922-104477153
Capsl	ENSMUSG00000039676	protein_coding	chr15:9365783-9395790
Ccdc152	ENSMUSG00000091119	protein_coding	chr15:3230627-3253526
Ccdc34	ENSMUSG00000027160	protein_coding	chr2:109857974-110013517
Cct8	ENSMUSG00000025613	protein_coding	chr16:87483571-87496118
Clec5a	ENSMUSG00000029915	protein_coding	chr6:40524893-40535820
Clstn2	ENSMUSG00000032452	protein_coding	chr9:97344814-97933600
Cmpk2	ENSMUSG00000020638	protein_coding	chr12:27154069-27164700
Commd6	ENSMUSG00000075486	protein_coding	chr14:102032983-102039903
Cpne4	ENSMUSG00000032564	protein_coding	chr9:104449616-104936874
D1Pas1	ENSMUSG00000039224	protein_coding	chr1:188791295-188794506
D7Ertd443e	ENSMUSG00000030994	protein_coding	chr7:141457945-141577344
Diap3	ENSMUSG00000022021	protein_coding	chr14:87055174-87541031
Dnahc9	ENSMUSG00000056752	protein_coding	chr11:65644784-65982053
<b>Dock1</b>	ENSMUSG00000058325	protein_coding	chr7:141862370-142365322
Dppa1	ENSMUSG00000064010	protein_coding	chr11:46421274-46442763
Dusp10	ENSMUSG00000039384	protein_coding	chr1:185837181-185899515
Dzip3	ENSMUSG00000064061	protein_coding	chr16:48924345-48994278

E030002O03Rik	ENSMUSG00000044265	protein_coding	chr7:111301527-111313345
Epb4.1I3	ENSMUSG00000024044	protein_coding	chr17:69506150-69639325
Esr1	ENSMUSG00000019768	protein_coding	chr10:5340927-5734948
<b>Esrrg</b>	ENSMUSG00000026610	protein_coding	chr1:189432670-190038764
Fam196a	ENSMUSG00000073805	protein_coding	chr7:142073609-142130113
Fam19a5	ENSMUSG00000054863	protein_coding	chr15:87374904-87589766
Fibin	ENSMUSG00000074971	protein_coding	chr2:110201082-110203150
Gcnt1	ENSMUSG00000038843	protein_coding	chr19:17400631-17431157
<b>Gfra2</b>	ENSMUSG00000022103	protein_coding	chr14:71289927-71379645
<b>Ghr</b>	ENSMUSG00000055737	protein_coding	chr15:3267760-3533492
Gm10097	ENSMUSG00000061261	protein_coding	chr10:5277031-5277348
Gm10240	ENSMUSG00000068397	protein_coding	chr15:68141381-68141863
Gm10290	ENSMUSG00000070408	protein_coding	chr5:28865060-28866308
Gm10610	ENSMUSG00000074038	protein_coding	chr7:90697653-90698138
Gm10852	ENSMUSG00000075532	protein_coding	chr2:10636794-10639296
Gm1153	ENSMUSG00000091137	protein_coding	chr8:57977384-57977890
Gm12169	ENSMUSG00000078924	protein_coding	chr11:46337714-46351658
Gm15217	ENSMUSG00000079261	protein_coding	chr14:46999089-47003283
Gm17293	ENSMUSG00000091502	protein_coding	chr8:57987540-57988046
Gm17662	ENSMUSG00000091038	protein_coding	chr4:104529934-104531742
Gm2832	ENSMUSG00000091110	protein_coding	chr14:42092094-42102104
Gm3486	ENSMUSG00000090505	protein_coding	chr14:42297521-42302774
Gm4222	ENSMUSG00000091703	protein_coding	chr2:89988617-89989045
Gm4511	ENSMUSG00000091746	protein_coding	chr12:33282246-33284111
Gm5434	ENSMUSG00000059301	protein_coding	chr12:36816966-36818416
Gm5798	ENSMUSG00000090345	protein_coding	chr14:42161898-42170128
Gm5848	ENSMUSG00000068979	protein_coding	chr3:68112747-68113103
Gm6132	ENSMUSG00000069200	protein_coding	chr13:70145574-70146603
Gm6482	ENSMUSG00000092142	protein_coding	chr14:42216174-42221570
Gm684	ENSMUSG00000079559	protein_coding	chr9:51078656-51080522
Gm7334	ENSMUSG00000044645	protein_coding	chr17:50837852-50839205
Gm7349	ENSMUSG00000091349	protein_coding	chr8:57980773-57981279
Gm7354	ENSMUSG00000091173	protein_coding	chr8:57984192-57984698
Gm7360	ENSMUSG00000090390	protein_coding	chr8:57990965-57991471
Gm7929	ENSMUSG00000091740	protein_coding	chr14:42044621-42048167
Gm7945	ENSMUSG00000091131	protein_coding	chr14:42194917-42199668

Gm7954	ENSMUSG00000091774	protein_coding	chr14:42261492-42266807
Gm7957	ENSMUSG00000090508	protein_coding	chr7:90560487-90560882
Gm8214	ENSMUSG00000090533	protein_coding	chr1:185505657-185506073
Gm826	ENSMUSG00000074623	protein_coding	chr2:160137129-160159898
Gm8906	ENSMUSG00000092089	protein_coding	chr5:11502685-11507417
Gm9866	ENSMUSG00000052076	protein_coding	chr12:27825667-27845311
Gm9922	ENSMUSG00000053821	protein_coding	chr14:102128597-102129031
Gpatch2	ENSMUSG00000039210	protein_coding	chr1:189039387-189175583
Gria1	ENSMUSG00000020524	protein_coding	chr11:56824889-57143746
Grin2b	ENSMUSG00000030209	protein_coding	chr6:135679844-136123529
<b>Hmgxb4</b>	ENSMUSG00000034518	protein_coding	chr8:77517255-77555877
Hmxo1	ENSMUSG00000005413	protein_coding	chr8:77617490-77624495
Igsf10	ENSMUSG00000036334	protein_coding	chr3:59120657-59148178
Il7r	ENSMUSG00000003882	protein_coding	chr15:9435916-9459631
Iqcj	ENSMUSG00000051777	protein_coding	chr3:67696142-67860515
Isx	ENSMUSG00000031621	protein_coding	chr8:77396618-77417405
Kcne4	ENSMUSG00000047330	protein_coding	chr1:78813502-78816599
Kirrel3	ENSMUSG00000032036	protein_coding	chr9:34293711-34844301
Lgr4	ENSMUSG00000050199	protein_coding	chr2:109757804-109854414
Lin7c	ENSMUSG00000027162	protein_coding	chr2:109731010-109741160
<b>Lmcd1</b>	ENSMUSG00000057604	protein_coding	chr6:112223752-112280419
<b>Lmo7</b>	ENSMUSG00000033060	protein_coding	chr14:102129145-102349230
Ltn1	ENSMUSG00000052299	protein_coding	chr16:87376896-87432851
Maf	ENSMUSG00000055435	protein_coding	chr8:118206842-118231694
<b>Map2k4</b>	ENSMUSG00000033352	protein_coding	chr11:65501745-65601799
Mat1a	ENSMUSG00000037798	protein_coding	chr14:41918670-41937701
Mbl1	ENSMUSG00000037780	protein_coding	chr14:41964745-41972248
Mcm5	ENSMUSG0000005410	protein_coding	chr8:77633427-77652338
Mon1b	ENSMUSG00000078908	protein_coding	chr8:116159850-116166305
Muc15	ENSMUSG00000050808	protein_coding	chr2:110561497-110579684
<b>Myocd</b>	ENSMUSG00000020542	protein_coding	chr11:64990063-65083491
N6amt1	ENSMUSG00000044442	protein_coding	chr16:87354430-87368987
<b>Ndrg1</b>	ENSMUSG00000005125	protein_coding	chr15:66760883-66801202
Ndufa4	ENSMUSG00000029632	protein_coding	chr6:11850373-11857446
Nps	ENSMUSG00000073804	protein_coding	chr7:142460302-142464625

<b>Nr3c1</b>	ENSMUSG00000024431	protein_coding	chr18:39570199-39650955
Ntf3	ENSMUSG00000049107	protein_coding	chr6:126051431-126116762
Obfc2a	ENSMUSG00000026107	protein_coding	chr1:51526342-51535243
Oca2	ENSMUSG00000030450	protein_coding	chr7:63495130-63791887
<b>Odz2</b>	ENSMUSG00000049336	protein_coding	chr11:35820158-37049466
Olfr1000	ENSMUSG00000075215	protein_coding	chr2:85448121-85449065
Olfr1002	ENSMUSG00000075214	protein_coding	chr2:85487520-85488476
Olfr1006	ENSMUSG00000075211	protein_coding	chr2:85514368-85518898
Olfr1012	ENSMUSG00000075210	protein_coding	chr2:85599596-85600531
Olfr1013	ENSMUSG00000053287	protein_coding	chr2:85609960-85610877
Olfr1014	ENSMUSG00000059379	protein_coding	chr2:85616743-85617660
Olfr1015	ENSMUSG00000033850	protein_coding	chr2:85625631-85626646
Olfr1016	ENSMUSG00000075209	protein_coding	chr2:85639496-85640425
Olfr1018	ENSMUSG00000043892	protein_coding	chr2:85663130-85664065
Olfr1019	ENSMUSG00000075208	protein_coding	chr2:85681014-85682393
Olfr1020	ENSMUSG00000046975	protein_coding	chr2:85689577-85690655
Olfr1022	ENSMUSG00000057761	protein_coding	chr2:85708751-85709698
Olfr1023	ENSMUSG00000050128	protein_coding	chr2:85726959-85728102
Olfr1024	ENSMUSG00000075206	protein_coding	chr2:85744226-85745209
Olfr1025-ps1	ENSMUSG00000058884	protein_coding	chr2:85758084-85759047
Olfr1026	ENSMUSG00000042863	protein_coding	chr2:85763427-85764350
Olfr1028	ENSMUSG00000057207	protein_coding	chr2:85791222-85792196
Olfr1029	ENSMUSG00000059873	protein_coding	chr2:85815370-85816430
Olfr1030	ENSMUSG00000044923	protein_coding	chr2:85819469-85824955
Olfr1031	ENSMUSG00000043267	protein_coding	chr2:85831976-85832986
Olfr1032	ENSMUSG00000042796	protein_coding	chr2:85847935-85848867
Olfr1254	ENSMUSG00000075074	protein_coding	chr2:89628563-89633327
Olfr1255	ENSMUSG00000045148	protein_coding	chr2:89656485-89657434
Olfr1256	ENSMUSG00000075073	protein_coding	chr2:89675180-89681290
Olfr1257	ENSMUSG00000049057	protein_coding	chr2:89718601-89721966
Olfr1258	ENSMUSG00000049149	protein_coding	chr2:89767476-89771002
Olfr1259	ENSMUSG00000068806	protein_coding	chr2:89783341-89784270
Olfr1260	ENSMUSG00000042894	protein_coding	chr2:89814866-89818869
Olfr1261	ENSMUSG00000061295	protein_coding	chr2:89831395-89834552
Olfr1262	ENSMUSG00000051313	protein_coding	chr2:89840302-89843527
Olfr1263	ENSMUSG00000059112	protein_coding	chr2:89855048-89856076
Olfr1264	ENSMUSG00000075069	protein_coding	chr2:89861295-89862221
Olfr1265	ENSMUSG00000059910	protein_coding	chr2:89877078-89878100
Olfr1269	ENSMUSG00000075067	protein_coding	chr2:89958757-89959774
Olfr1270	ENSMUSG00000075065	protein_coding	chr2:89989176-89990193
Olfr140	ENSMUSG00000075068	protein_coding	chr2:899891571-89903751
Olfr154	ENSMUSG00000075212	protein_coding	chr2:85503534-85504612
Olfr32	ENSMUSG00000075066	protein_coding	chr2:89978345-89979352
Olfr460	ENSMUSG00000045514	protein_coding	chr6:40521356-40522416
Olfr48	ENSMUSG00000075072	protein_coding	chr2:89684223-89685128
Olfr640	ENSMUSG00000066262	protein_coding	chr7:111169886-111170830
Olfr641	ENSMUSG00000073932	protein_coding	chr7:111188312-111189250
Olfr642	ENSMUSG00000049797	protein_coding	chr7:111197922-111198866
Olfr643	ENSMUSG00000058621	protein_coding	chr7:111207170-111208114
Olfr644	ENSMUSG00000062172	protein_coding	chr7:111216599-111217543

Olfr645	ENSMUSG00000051340	protein_coding	chr7:111232557-111233689
Olfr646	ENSMUSG00000073931	protein_coding	chr7:111254795-111255733
Olfr648	ENSMUSG00000042909	protein_coding	chr7:111327970-111328920
Olfr649	ENSMUSG00000044899	protein_coding	chr7:111337780-111344474
Olfr681	ENSMUSG00000073911	protein_coding	chr7:112269969-112270920
Olfr682-ps1	ENSMUSG00000059768	protein_coding	chr7:112274886-112276919
Olfr683	ENSMUSG00000044120	protein_coding	chr7:112291864-112292823
Olfr684	ENSMUSG00000047225	protein_coding	chr7:112305081-112306194
Olfr685	ENSMUSG00000047794	protein_coding	chr7:112328827-112329914
Olfr686	ENSMUSG00000048425	protein_coding	chr7:112351873-112352890
Olfr687	ENSMUSG00000073908	protein_coding	chr7:112424031-112424945
Olfr688	ENSMUSG00000073909	protein_coding	chr7:112436609-112437574
Olfr689	ENSMUSG00000073907	protein_coding	chr7:112462496-112463571
Olfr748	ENSMUSG00000060084	protein_coding	chr14:51330007-51330930
Olfr987	ENSMUSG00000075223	protein_coding	chr2:85171054-85179452
Olfr988	ENSMUSG00000075222	protein_coding	chr2:85193082-85203215
Olfr992	ENSMUSG00000075221	protein_coding	chr2:85239759-85240688
Olfr993	ENSMUSG00000075220	protein_coding	chr2:85254090-85255034
Olfr994	ENSMUSG00000075219	protein_coding	chr2:85270040-85270984
Olfr995	ENSMUSG00000075218	protein_coding	chr2:85278282-85279394
Olfr996	ENSMUSG00000059990	protein_coding	chr2:85419372-85420439
Olfr998	ENSMUSG00000046076	protein_coding	chr2:85430667-85431678
ORF63	ENSMUSG00000025610	protein_coding	chr16:87553575-87595581
Otol1	ENSMUSG00000027788	protein_coding	chr3:69811535-69832630
<b>Palmd</b>	ENSMUSG00000033377	protein_coding	chr3:116621174-116671905
Penk	ENSMUSG00000045573	protein_coding	chr4:4060678-4065966
Phf14	ENSMUSG00000029629	protein_coding	chr6:11857809-12031197
Plcl2	ENSMUSG00000038910	protein_coding	chr17:50648872-50827818
<b>Pld1</b>	ENSMUSG00000027695	protein_coding	chr3:27837602-28032284
<b>Plxna4</b>	ENSMUSG00000029765	protein_coding	chr6:32094565-32538192
Pou2af1	ENSMUSG00000032053	protein_coding	chr9:51021795-51048184
Prl3d3	ENSMUSG00000062201	protein_coding	chr13:27248659-27254459
<b>Prune2</b>	ENSMUSG00000039126	protein_coding	chr19:17030608-17298422
<b>Ptger3</b>	ENSMUSG00000040016	protein_coding	chr3:157229856-157307722
Rasd2	ENSMUSG00000034472	protein_coding	chr8:77737843-77748012
Rfk	ENSMUSG00000024712	protein_coding	chr19:17468533-17475839
Rgs7bp	ENSMUSG00000021719	protein_coding	chr13:105737233-105845010

Rnf144a	ENSMUSG00000020642	protein_coding	chr12:26991662-27100121
Rorb	ENSMUSG00000036192	protein_coding	chr19:19005095-19185686
Rpl13-ps3	ENSMUSG00000059835	protein_coding	chr14:59512343-59512966
Rpl21-ps10	ENSMUSG00000064315	protein_coding	chr3:38006330-38006877
Rpl31-ps4	ENSMUSG00000090753	protein_coding	chr16:87549307-87549696
Rrp15	ENSMUSG0000001305	protein_coding	chr1:188544857-188573237
Rсад2	ENSMUSG00000020641	protein_coding	chr12:27127618-27141317
Rwdd2b	ENSMUSG00000041079	protein_coding	chr16:87433652-87440818
Sdr16c5	ENSMUSG00000028236	protein_coding	chr4:3923083-3946810
Sdr16c6	ENSMUSG00000071019	protein_coding	chr4:3983078-4004669
Sepp1	ENSMUSG00000064373	protein_coding	chr15:3218547-3230508
Sftpa1	ENSMUSG00000021789	protein_coding	chr14:41945071-41949741
Sftpd	ENSMUSG00000021795	protein_coding	chr14:41985501-41998487
Shisa6	ENSMUSG00000053930	protein_coding	chr11:66025227-66339466
Sla	ENSMUSG00000022372	protein_coding	chr15:66612381-66663391
Slc2a2	ENSMUSG00000027690	protein_coding	chr3:28596825-28627278
Slc5a12	ENSMUSG00000041644	protein_coding	chr2:110437455-110487936
Snai2	ENSMUSG00000022676	protein_coding	chr16:14705945-14709488
Sntg2	ENSMUSG00000020672	protein_coding	chr12:30859347-31058240
<b>Sox11</b>	ENSMUSG00000063632	protein_coding	chr12:28025562-28027574
Spata17	ENSMUSG00000026611	protein_coding	chr1:188868527-189039344
St3gal1	ENSMUSG00000013846	protein_coding	chr15:66934437-66945922
Syce1l	ENSMUSG00000033409	protein_coding	chr8:116167113-116179433
<b>Syne1</b>	ENSMUSG00000019769	protein_coding	chr10:4795849-5326338
Tas2r138	ENSMUSG00000058250	protein_coding	chr6:40562314-40563309
<b>Tbc1d4</b>	ENSMUSG00000033083	protein_coding	chr14:101841577-102008408
Tcerg1l	ENSMUSG00000091002	protein_coding	chr7:145400657-145589413
Tdrd3	ENSMUSG00000022019	protein_coding	chr14:87816390-87945315
Tg	ENSMUSG00000053469	protein_coding	chr15:66502315-66682283
Timd2	ENSMUSG00000040413	protein_coding	chr11:46482462-46520563
Tmem18	ENSMUSG00000043061	protein_coding	chr12:31269308-31276078
Tmem212	ENSMUSG00000043164	protein_coding	chr3:27764988-27795290
Tnik	ENSMUSG00000027692	protein_coding	chr3:28162136-28574780
Tom1	ENSMUSG00000042870	protein_coding	chr8:77557585-77594020

Tpo	ENSMUSG00000020673	protein_coding	chr12:30739524-30817489
Trim12a	ENSMUSG00000066258	protein_coding	chr7:111448408-111463980
Trim12c	ENSMUSG00000057143	protein_coding	chr7:111487268-111501876
Trim34a	ENSMUSG00000056144	protein_coding	chr7:111392971-111489207
Trim34b	ENSMUSG00000090215	protein_coding	chr7:111448744-111485423
Trim42	ENSMUSG00000032451	protein_coding	chr9:97249981-97270377
Trim5	ENSMUSG00000060441	protein_coding	chr7:111411900-111436608
Trim6	ENSMUSG00000072244	protein_coding	chr7:111367307-111383666
Tspan13	ENSMUSG00000020577	protein_coding	chr12:36741144-36769087
Ubqln3	ENSMUSG00000051618	protein_coding	chr7:111289137-111291793
Ubqlnl	ENSMUSG00000051437	protein_coding	chr7:111296773-111299070
Uchl3	ENSMUSG00000022111	protein_coding	chr14:102053184-102095341
Ush2a	ENSMUSG00000026609	protein_coding	chr1:190085902-190788920
Usp16	ENSMUSG00000025616	protein_coding	chr16:87454948-87483762
<b>Wisp1</b>	ENSMUSG00000005124	protein_coding	chr15:66722882-66754763
Xylt1	ENSMUSG00000030657	protein_coding	chr7:124524493-124811265
Zfat	ENSMUSG00000022335	protein_coding	chr15:67915328-68090418
<b>Zfp161</b>	ENSMUSG00000049672	protein_coding	chr17:69732390-69740090
Zkscan6	ENSMUSG00000018347	protein_coding	chr11:65620677-65642741
Zranb2	ENSMUSG00000028180	protein_coding	chr3:157197124-157211354
Zscan4-ps2	ENSMUSG00000070826	protein_coding	chr7:12099659-12104460
Zscan4c	ENSMUSG00000054272	protein_coding	chr7:11591071-11595896
Zscan4d	ENSMUSG00000090714	protein_coding	chr7:11746992-11751497
Zscan4e	ENSMUSG00000091880	protein_coding	chr7:11891727-11896031
Zscan4f	ENSMUSG00000070828	protein_coding	chr7:11983264-11988090

**Table S7. Genes within shared H3K9me2 domains lost in D3 DMSO and D3 RA**

SYMBOL	ENSEMBL	biotype	gene location
1700011I03Rik	ENSMUSG00000058925	protein_coding	chr18:57693434-57890719
1700017N19Rik	ENSMUSG00000056912	protein_coding	chr10:100055020-100081025
4921522P10Rik	ENSMUSG00000040467	protein_coding	chr8:8661801-8664728
4930430F08Rik	ENSMUSG00000046567	protein_coding	chr10:100034908-100051893
4930579G24Rik	ENSMUSG00000027811	protein_coding	chr3:79433001-79436739
4930589L23Rik	ENSMUSG00000068957	protein_coding	chr3:79372114-79376502
4930597O21Rik	ENSMUSG00000053442	protein_coding	chr6:66844648-66846515

5730469M10Rik	ENSMUSG00000021792	protein_coding	chr14:41807029-41827077
9630041A04Rik	ENSMUSG00000057710	protein_coding	chr9:101840811-101845549
A930011G23Rik	ENSMUSG00000089809	protein_coding	chr5:99726263-100158084
Abcd2	ENSMUSG00000055782	protein_coding	chr15:90976315-91022238
Adam12	ENSMUSG00000054555	protein_coding	chr7:141074882-141423829
Agtr1a	ENSMUSG00000049115	protein_coding	chr13:30428310-30474736
AI427809	ENSMUSG00000073854	protein_coding	chr4:53274765-53275419
Ankrd13c	ENSMUSG00000039988	protein_coding	chr3:157610378-157670288
Arglu1	ENSMUSG00000040459	protein_coding	chr8:8666577-8690537
Arhgap24	ENSMUSG00000057315	protein_coding	chr5:102910410-103326955
Arhgap44	ENSMUSG00000033389	protein_coding	chr11:64815541-64976463
Armc4	ENSMUSG00000061802	protein_coding	chr18:7088231-7297899
Asap1	ENSMUSG00000022377	protein_coding	chr15:63918419-64214481
Atp2b1	ENSMUSG00000019943	protein_coding	chr10:98377786-98488777
Atp5j	ENSMUSG00000022890	protein_coding	chr16:84828111-84835870
B4galt6	ENSMUSG00000056124	protein_coding	chr18:20843100-20904905
B530045E10Rik	ENSMUSG00000044633	protein_coding	chr10:98883156-98885681
Bcl6	ENSMUSG00000022508	protein_coding	chr16:23965138-23988938
Cdh6	ENSMUSG00000039385	protein_coding	chr15:12963955-13103394
Cep290	ENSMUSG00000019971	protein_coding	chr10:99950923-100036289
Chrm3	ENSMUSG00000046159	protein_coding	chr13:9876381-9878329
CN725425	ENSMUSG00000078932	protein_coding	chr15:91062009-91091316
Crim1	ENSMUSG00000024074	protein_coding	chr17:78599588-78775932
Cth	ENSMUSG00000028179	protein_coding	chr3:157557212-157588041
Ctxn3	ENSMUSG00000069372	protein_coding	chr18:57628140-57637788
Dsg2	ENSMUSG00000044393	protein_coding	chr18:20716575-20763022
Dusp22	ENSMUSG00000069255	protein_coding	chr13:30751868-30803100
Dusp6	ENSMUSG00000019960	protein_coding	chr10:98725865-98730122
Dydc1	ENSMUSG00000021790	protein_coding	chr14:41886200-41905482
Dydc2	ENSMUSG00000021791	protein_coding	chr14:41862498-41882497
Efnb2	ENSMUSG00000001300	protein_coding	chr8:8617434-8661239
Eif5a2	ENSMUSG00000050192	protein_coding	chr3:28680233-28697768

Elac2	ENSMUSG00000020549	protein_coding	chr11:64792540-64815571
Ephb1	ENSMUSG00000032537	protein_coding	chr9:101824458-102257023
Etfdh	ENSMUSG00000027809	protein_coding	chr3:79407710-79432785
Exoc2	ENSMUSG00000021357	protein_coding	chr13:30905788-31065916
Fam198b	ENSMUSG00000027955	protein_coding	chr3:79688455-79750202
Fam49b	ENSMUSG00000022378	protein_coding	chr15:63760652-63892010
Fga	ENSMUSG00000028001	protein_coding	chr3:82830075-82838036
Fgb	ENSMUSG00000033831	protein_coding	chr3:82846169-82853725
Fgg	ENSMUSG00000033860	protein_coding	chr3:82811781-82818975
Fndc3b	ENSMUSG00000039286	protein_coding	chr3:27315084-27610229
Fnip2	ENSMUSG00000061175	protein_coding	chr3:79259893-79371718
Frem3	ENSMUSG00000042353	protein_coding	chr8:83134938-83219370
Frrs1	ENSMUSG00000033386	protein_coding	chr3:116581145-116606668
Gabpa	ENSMUSG00000008976	protein_coding	chr16:84835170-84864024
Gad1-ps	ENSMUSG00000090665	protein_coding	chr10:98906364-98909641
Gadl1	ENSMUSG00000056880	protein_coding	chr9:115817682-115985294
Galnt4	ENSMUSG00000090035	protein_coding	chr10:98570793-98575881
Glis3	ENSMUSG00000052942	protein_coding	chr19:28333341-28754567
Glis3	ENSMUSG00000091294	protein_coding	chr19:28336916-28374868
Gm10217	ENSMUSG00000067627	protein_coding	chr8:9864251-9870315
Gm10258	ENSMUSG00000069074	protein_coding	chr3:30166747-30168869
Gm10269	ENSMUSG00000091449	protein_coding	chr18:20841060-20841504
Gm10710	ENSMUSG00000074517	protein_coding	chr3:82929198-82933168
Gm17359	ENSMUSG00000091685	protein_coding	chr3:79149298-79268051
Gm17485	ENSMUSG00000090783	protein_coding	chr3:28694778-28701145
Gm17728	ENSMUSG00000072968	protein_coding	chr17:9614925-9615323
Gm5160	ENSMUSG00000055795	protein_coding	chr18:14582159-14583820
Gm5447	ENSMUSG00000056257	protein_coding	chr13:31066073-31067845
Gm6457	ENSMUSG00000053740	protein_coding	chr18:14728622-14730186
Gm6505	ENSMUSG00000070522	protein_coding	chr3:28662453-28664314
Gm6816	ENSMUSG00000046411	protein_coding	chr7:122070473-122071240
Gm9762	ENSMUSG00000037096	protein_coding	chr3:78770278-78770721
Gpr171	ENSMUSG00000050075	protein_coding	chr3:58900370-58905743
Gpr87	ENSMUSG00000051431	protein_coding	chr3:58982845-58999026
Grxcr1	ENSMUSG00000068082	protein_coding	chr5:68423074-68557637
Gsdmc	ENSMUSG00000079025	protein_coding	chr15:63607526-63640314
Gsdmc2	ENSMUSG00000056293	protein_coding	chr15:63655901-63667504
Gsdmc3	ENSMUSG00000055827	protein_coding	chr15:63689826-63700852

Gsdmc4	ENSMUSG00000055748	protein_coding	chr15:63722820-63734491
Gsdmcl1	ENSMUSG00000062543	protein_coding	chr15:63678864-63682497
Gypa	ENSMUSG00000051839	protein_coding	chr8:83017944-83034684
Hs3st3a1	ENSMUSG00000047759	protein_coding	chr11:64248834-64336343
Hus1b	ENSMUSG00000076430	protein_coding	chr13:31038442-31039628
Icos	ENSMUSG00000026009	protein_coding	chr1:61034771-61057164
Insc	ENSMUSG00000048782	protein_coding	chr7:121887208-121993894
Irf4	ENSMUSG00000021356	protein_coding	chr13:30841095-30858796
Itgb6	ENSMUSG00000026971	protein_coding	chr2:60436349-60560700
Jam2	ENSMUSG00000053062	protein_coding	chr16:84774368-84826173
Kcnk9	ENSMUSG00000036760	protein_coding	chr15:72342549-72376709
Lhcgr	ENSMUSG00000024107	protein_coding	chr17:89140889-89191316
Lrat	ENSMUSG00000028003	protein_coding	chr3:82696501-82707895
Lrrc40	ENSMUSG00000063052	protein_coding	chr3:157699626-157731442
Lrrk2	ENSMUSG00000036273	protein_coding	chr15:91503606-91646551
Lyzl1	ENSMUSG00000024233	protein_coding	chr18:4165830-4182230
Masp1	ENSMUSG00000022887	protein_coding	chr16:23449490-23520676
Mecom	ENSMUSG00000027684	protein_coding	chr3:29850221-30446930
Mep1b	ENSMUSG00000024313	protein_coding	chr18:21229286-21258700
Mitf	ENSMUSG00000035158	protein_coding	chr6:97757052-97971352
Mkx	ENSMUSG00000061013	protein_coding	chr18:6934998-7004724
Milt3	ENSMUSG00000028496	protein_coding	chr4:87415829-87679268
Mrpl39	ENSMUSG00000022889	protein_coding	chr16:84717821-84735987
Muc19	ENSMUSG00000044021	protein_coding	chr15:91668757-91766819
Nek7	ENSMUSG00000026393	protein_coding	chr1:140381291-140516273
Nmur2	ENSMUSG00000037393	protein_coding	chr11:55838489-55854512
Npas3	ENSMUSG00000021010	protein_coding	chr12:54349664-55173162
Nxph2	ENSMUSG00000069132	protein_coding	chr2:23176766-23257493
Olfr1008	ENSMUSG00000050603	protein_coding	chr2:85529588-85530529
Olfr1009	ENSMUSG00000043226	protein_coding	chr2:85561564-85562508
Olfr3	ENSMUSG00000075384	protein_coding	chr2:36667669-36668610
Olfr340	ENSMUSG00000058803	protein_coding	chr2:36308107-36309045
Olfr341	ENSMUSG00000075387	protein_coding	chr2:36334707-36335648
Olfr342	ENSMUSG00000061305	protein_coding	chr2:36382908-36383961
Olfr344	ENSMUSG00000058205	protein_coding	chr2:36424120-36425049
Olfr345	ENSMUSG00000059251	protein_coding	chr2:36495561-36496496
Olfr346	ENSMUSG00000063915	protein_coding	chr2:36543524-36544453
Olfr347	ENSMUSG00000057351	protein_coding	chr2:36589839-36590781
Olfr348	ENSMUSG00000049315	protein_coding	chr2:36639796-36642988
Olfr350	ENSMUSG00000050015	protein_coding	chr2:36705568-36706506

Olfr351	ENSMUSG00000075383	protein_coding	chr2:36714934-36715866
Olfr352	ENSMUSG00000053146	protein_coding	chr2:36725088-36726035
Olfr353	ENSMUSG00000075382	protein_coding	chr2:36745431-36746366
Olfr354	ENSMUSG00000055088	protein_coding	chr2:36762431-36763514
Olfr355	ENSMUSG00000075380	protein_coding	chr2:36782700-36783632
Olfr356	ENSMUSG00000070943	protein_coding	chr2:36792641-36793588
Olfr357	ENSMUSG00000055838	protein_coding	chr2:36852247-36853338
Olfr358	ENSMUSG00000075379	protein_coding	chr2:36860109-36861167
Olfr360	ENSMUSG00000083361	protein_coding	chr2:36921266-36924780
Olfr361	ENSMUSG00000075378	protein_coding	chr2:36940298-36941266
Olfr362	ENSMUSG00000075377	protein_coding	chr2:36960215-36961168
Olfr364-ps1	ENSMUSG00000078198	protein_coding	chr2:37001734-37002657
Olfr365	ENSMUSG00000059429	protein_coding	chr2:37056763-37057701
Olfr366	ENSMUSG00000068947	protein_coding	chr2:37075011-37075940
Olfr50	ENSMUSG00000061900	protein_coding	chr2:36648758-36649888
P2ry12	ENSMUSG00000036353	protein_coding	chr3:59020193-59066753
P2ry13	ENSMUSG00000036362	protein_coding	chr3:59011818-59014804
P2ry14	ENSMUSG00000036381	protein_coding	chr3:58918548-58934546
Pabpc6	ENSMUSG00000046173	protein_coding	chr17:9859362-9862569
Pard3	ENSMUSG00000025812	protein_coding	chr8:129587793-130136186
Phxr2	ENSMUSG00000055108	protein_coding	chr10:98588151-98588955
Pik3c2g	ENSMUSG00000030228	protein_coding	chr6:139570409-139916464
Pik3cg	ENSMUSG00000020573	protein_coding	chr12:32858338-32893524
Plrg1	ENSMUSG00000027998	protein_coding	chr3:82859444-82876277
Plxna2	ENSMUSG00000026640	protein_coding	chr1:196446023-196643063
Poc1b	ENSMUSG00000019952	protein_coding	chr10:98569670-98660708
Ppid	ENSMUSG00000027804	protein_coding	chr3:79395264-79407572
Rapgef2	ENSMUSG00000062232	protein_coding	chr3:78866438-78985262
Rasgef1b	ENSMUSG00000029333	protein_coding	chr5:99646445-99681946
Rbms1	ENSMUSG00000026970	protein_coding	chr2:60588250-60801261
Rfx3	ENSMUSG00000040929	protein_coding	chr19:27836211-28085656
Rnf125	ENSMUSG00000033107	protein_coding	chr18:21103126-21142349
Rnf138	ENSMUSG00000024317	protein_coding	chr18:21159842-21186724
Rnf32	ENSMUSG00000029130	protein_coding	chr5:29522532-29552064
Rora	ENSMUSG00000032238	protein_coding	chr9:68501593-69236053
Rpl22l1	ENSMUSG00000039221	protein_coding	chr3:28704358-28706274
Rtp1	ENSMUSG00000033383	protein_coding	chr16:23429206-23434033
Rtp2	ENSMUSG00000047531	protein_coding	chr16:23925634-23930873
Rtp4	ENSMUSG00000033355	protein_coding	chr16:23610005-23614308
Rxfp1	ENSMUSG00000034009	protein_coding	chr3:79448638-79541716
Sh2d4b	ENSMUSG00000037833	protein_coding	chr14:41627078-41706555
Slc12a2	ENSMUSG00000024597	protein_coding	chr18:58038332-58106475
Slc24a2	ENSMUSG00000037996	protein_coding	chr4:86629028-86876381

Slc2a13	ENSMUSG00000036298	protein_coding	chr15:91098122-91403692
Slc35b3	ENSMUSG00000021432	protein_coding	chr13:39024009-39052744
Smgc	ENSMUSG00000047295	protein_coding	chr15:91668696-91691869
Sox5	ENSMUSG00000041540	protein_coding	chr6:143776945-144730497
Sox6	ENSMUSG00000051910	protein_coding	chr7:122614858-123182258
Spag17	ENSMUSG00000027867	protein_coding	chr3:99689329-99947245
Srsf11	ENSMUSG00000055436	protein_coding	chr3:157673437-157699603
Sst	ENSMUSG00000004366	protein_coding	chr16:23889667-23890930
Tgfbr2	ENSMUSG00000032440	protein_coding	chr9:115993415-116084383
Tmem144	ENSMUSG00000027956	protein_coding	chr3:79617070-79646584
Tmtc3	ENSMUSG00000036676	protein_coding	chr10:99906536-99949984
Tnp1	ENSMUSG00000026182	protein_coding	chr1:73061657-73062473
Trappc8	ENSMUSG00000033382	protein_coding	chr18:20975725-21054579
Tspan14	ENSMUSG00000037824	protein_coding	chr14:41719734-41780096
Ttr	ENSMUSG00000061808	protein_coding	chr18:20823751-20832825
Uqcrfs1	ENSMUSG00000038462	protein_coding	chr13:30632177-30637231
Zcwpw2	ENSMUSG00000032443	protein_coding	chr9:117856918-117923278
Zfp521	ENSMUSG00000024420	protein_coding	chr18:13845522-14131242

**Table S8. Fold Change of D3 RA in RA-specific domain loss**

ENSEMBL	SYMBOL	Log <sub>2</sub> FC	adj.P.Val	Regulation
ENSMUSG00000042834	D0H4S114	3.937831035	3.32E-14	up
ENSMUSG00000017491	Rarb	6.656339146	3.42E-14	up
ENSMUSG00000024501	Dpysl3	2.901480587	9.35E-13	up
ENSMUSG00000029838	Ptn	3.949239924	2.08E-12	up
ENSMUSG00000050334	C130071C03Rik	6.588865672	1.43E-12	up
ENSMUSG00000027684	Mecom	3.08799711	2.62E-12	up
ENSMUSG00000047261	Gap43	2.925640435	3.15E-12	up
ENSMUSG00000049001	A930038C07Rik	6.346209198	1.56E-11	up
ENSMUSG00000020601	Trib2	1.643630259	5.91E-11	up
ENSMUSG00000025810	Nrp1	5.107007587	5.97E-11	up
ENSMUSG00000015243	Abca1	3.098067416	2.09E-10	up
ENSMUSG00000052062	Pard3b	3.534599484	2.08E-10	up
ENSMUSG00000090386	2810055G20Rik	8.563780949	3.91E-11	up
ENSMUSG00000036478	Btg1	1.966644197	3.29E-10	up
ENSMUSG00000022454	Nell2	2.484325599	3.79E-10	up
ENSMUSG00000087060	2810442I21Rik	2.509494678	3.03E-09	up
ENSMUSG00000027955	Fam198b	1.568414658	4.26E-09	up
ENSMUSG00000029534	St7	1.643295526	1.53E-08	up
ENSMUSG00000038128	Camk4	3.100656945	2.36E-08	up
ENSMUSG00000040943	Tet2	1.625433023	2.05E-08	up
ENSMUSG00000052450	2810055G20Rik	5.380783621	2.86E-08	up

ENSMUSG00000005583	Mef2c	2.244735009	1.58E-07	up
ENSMUSG00000038349	Plcl1	5.120614629	1.75E-07	up
ENSMUSG00000042514	Klhl14	3.467613594	8.80E-06	up
ENSMUSG00000019966	Kitl	2.087902666	8.46E-06	up
ENSMUSG00000063600	Egfem1	2.094572278	1.10E-05	up
ENSMUSG00000087565	Gm14662	4.151545355	1.86E-05	up
ENSMUSG00000053025	Sv2b	2.597540268	4.99E-05	up
ENSMUSG0000007655	Cav1	2.32538	0.000249225	up
ENSMUSG00000066842	Hmcn1	1.502634049	0.000224381	up
ENSMUSG00000065855	U6	2.02647591	0.000564558	up
ENSMUSG00000043518	Rai2	2.478013225	0.001257413	up
ENSMUSG00000040569	Slc26a7	1.556181222	0.001431909	up
ENSMUSG00000052560	Cpne8	1.768811379	0.005379915	up
ENSMUSG00000031139	Mcf2	-2.68647091	3.26E-08	down
		-		
ENSMUSG00000022367	Has2	1.682090459	7.13E-08	down
ENSMUSG00000054951	9130008F23Rik	-1.69351084	0.021692171	down
ENSMUSG00000022892	App	1.287294116	1.38E-10	no change
ENSMUSG00000017485	Top2b	0.901698055	1.82E-09	no change
ENSMUSG00000029910	Mad2l1	0.945251193	3.30E-09	no change
ENSMUSG00000022338	Eny2	1.0388491	8.84E-09	no change
ENSMUSG00000035762	Tmem161b	1.169281233	3.32E-08	no change
ENSMUSG00000023919	Cenpq	1.13736066	3.11E-08	no change
		-		
ENSMUSG00000020116	Pno1	0.793735204	3.29E-08	no change
ENSMUSG00000067870	Gm8759	0.921425107	1.17E-07	no change
ENSMUSG00000022867	Usp25	0.773864856	2.08E-07	no change
ENSMUSG00000062949	Atp11c	1.099040009	3.75E-07	no change
ENSMUSG00000029552	Tes	0.96181781	4.22E-07	no change
		-		
ENSMUSG00000024642	Tle4	0.846959115	4.07E-07	no change
ENSMUSG00000053477	Tcf4	1.084987946	4.89E-07	no change
ENSMUSG00000090744	Gm6871	-1.48616369	1.00E-06	no change
ENSMUSG00000022629	Kif21a	0.74096316	7.87E-07	no change
ENSMUSG00000053819	Camk2d	0.724895896	1.31E-06	no change
ENSMUSG00000020948	Klhl28	1.181980645	3.44E-06	no change
ENSMUSG00000022865	Cxadr	0.636614595	2.10E-06	no change
		-		
ENSMUSG00000057147	Atpbd4	0.875526739	3.27E-06	no change
ENSMUSG00000015247	Nipsnap3b	0.798419982	2.90E-06	no change
ENSMUSG00000035597	Prpf39	0.509740562	4.26E-06	no change
ENSMUSG00000020949	Fkbp3	0.692351029	3.64E-06	no change
		-		
ENSMUSG00000028018	Gstcd	0.763669329	6.28E-06	no change
ENSMUSG00000043424	Gm9781	-0.83271827	7.97E-06	no change
ENSMUSG00000047534	Mis18bp1	0.522133846	7.95E-06	no change
ENSMUSG00000029569	Tmem168	0.604364179	1.08E-05	no change
ENSMUSG00000045179	Sox3	0.913556246	1.48E-05	no change
		-		
ENSMUSG0000006005	Tpr	0.472889193	1.73E-05	no change
ENSMUSG00000022312	Eif3h	0.507750503	1.95E-05	no change
ENSMUSG00000048188	Gm8181	0.948120645	4.60E-05	no change
		-		
ENSMUSG0000006586	Runx1t1	0.754112523	3.34E-05	no change
ENSMUSG00000026771	Spopl	0.545194469	5.99E-05	no change
ENSMUSG0000006010	BC003331	0.54687766	5.93E-05	no change
ENSMUSG00000020122	Egfr	1.083209252	0.000140466	no change

ENSMUSG00000059493	Nhs	-0.975450847	0.000124277	no change
ENSMUSG00000033953	Ppp3r1	-0.423333303	8.32E-05	no change
ENSMUSG00000022708	Zbtb20	1.202202055	0.00033161	no change
ENSMUSG00000021785	Ngly1	0.903621787	0.000311328	no change
ENSMUSG00000022314	Rad21	0.264693884	0.000198527	no change
ENSMUSG00000047227	Gm527	1.443852979	0.000896491	no change
ENSMUSG00000048490	Nrip1	0.696762139	0.000332505	no change
ENSMUSG00000028016	Ints12	0.477018509	0.000381903	no change
ENSMUSG00000075470	Alg10b	0.514204996	0.000330394	no change
ENSMUSG00000029090	Gpr125	0.444475574	0.000390386	no change
ENSMUSG00000029913	Prdm5	1.006846851	0.001392658	no change
ENSMUSG00000000581	C1d	0.516161637	0.000587688	no change
ENSMUSG00000050299	Gm9843	0.487789255	0.000561414	no change
ENSMUSG00000028030	Tbck	0.555293628	0.001172667	no change
ENSMUSG00000028184	Lphn2	-0.819201226	0.000764673	no change
ENSMUSG00000039954	Stk32a	0.838138475	0.002053123	no change
ENSMUSG00000022863	Btg3	-1.262058025	0.004933023	no change
ENSMUSG00000009376	Met	0.613318766	0.002506897	no change
ENSMUSG00000028013	Ppa2	0.386391482	0.002623486	no change
ENSMUSG00000020120	Plek	1.184363292	0.007147541	no change
ENSMUSG00000021549	Rasa1	0.28287103	0.002664368	no change
ENSMUSG00000044966	Fbxo48	0.78872317	0.008762194	no change
ENSMUSG00000039782	Cpeb2	1.037906749	0.00859073	no change
ENSMUSG00000079157	Fam155a	1.197431525	0.012846238	no change
ENSMUSG00000040998	Nppt	0.916461902	0.01178315	no change
ENSMUSG00000015733	Capza2	0.194093225	0.007073185	no change
ENSMUSG00000024378	Stard4	0.555262277	0.010839307	no change
ENSMUSG00000044629	Cnrip1	-0.400194978	0.023028216	no change
ENSMUSG00000074166	AW146154	0.352719211	0.039287277	no change
ENSMUSG00000026986	Hnmt	0.751777518	0.088005449	no change
ENSMUSG00000055884	Fancm	-0.296226087	0.031008389	no change
ENSMUSG00000040282	BC052040	-0.462139464	0.064838919	no change
ENSMUSG00000021786	Oxsm	-0.558630885	0.124282803	no change
ENSMUSG00000035614	Fam179b	0.203192831	0.038457398	no change
ENSMUSG00000042680	Fam59a	-0.330636421	0.091150038	no change
ENSMUSG00000055370	Gm9968	0.248815419	0.745428313	no change
ENSMUSG00000071273	Gm5145	-0.334913206	0.397208203	no change
ENSMUSG00000006014	Prg4	-0.402610245	0.441767613	no change
ENSMUSG00000028221	Tmem55a	0.176411097	0.096625985	no change
ENSMUSG00000046934	Csl	0.266145153	0.261637705	no change
ENSMUSG00000064325	Hhip	0.274228809	0.554815854	no change
ENSMUSG00000028029	Aimp1	0.174049849	0.109594612	no change
ENSMUSG00000078974	Sec61g	0.130439538	0.696038533	no change
ENSMUSG00000042742	B630005N14Rik	-0.146876718	0.261801603	no change

ENSMUSG00000024502	Jakmip2	0.100960957	0.4119894	no change
ENSMUSG00000078970	Wdr92	-0.11116014	0.364381946	no change
ENSMUSG00000022864	D16Ertd472e	0.052281192	0.76241131	no change
ENSMUSG00000022313	Utp23	-0.003394488	0.982932668	no change
ENSMUSG00000079575	Rbpsuh-rs3	0.061062351	0.655411216	no change
ENSMUSG00000040550	Otud6b	0.075973884	0.411565648	no change
ENSMUSG00000023921	Mut	0.079659352	0.518467498	no change
ENSMUSG00000021548	Ccnh	-0.053930688	0.590358125	no change

**Table S9. Fold Change of D3 DMSO in DMSO-specific domain loss**

ENSEMBL	SYMBOL	Log <sub>2</sub> FC	adj.P.Val	Regulation
ENSMUSG00000042659	Arrdc4	2.385326213	7.56E-11	up
ENSMUSG00000074968	Ano3	3.733987005	8.29E-09	up
ENSMUSG00000021536	Adcy2	3.496681591	2.33E-08	up
ENSMUSG00000029765	Plxna4	2.264465806	2.51E-06	up
ENSMUSG00000056752	Dnahc9	3.129739101	4.38E-05	up
ENSMUSG00000050199	Lgr4	-1.504389652	1.35E-10	down
ENSMUSG00000045573	Penk	-2.434373435	2.11E-07	down
ENSMUSG00000091002	Tcerg1l	-3.165508558	3.06E-07	down
ENSMUSG00000053930	Shisa6	-1.991348727	0.000105046	down
ENSMUSG00000020524	Gria1	-3.493596454	0.00016274	down
ENSMUSG00000038843	Gcnt1	1.197743207	1.98E-08	no change
ENSMUSG00000055737	Ghr	1.427469248	1.73E-07	no change
ENSMUSG00000043061	Tmem18	0.939846917	2.71E-07	no change
ENSMUSG00000057143	Trim12c	1.239662284	2.98E-07	no change
ENSMUSG00000022019	Tdrd3	0.890583271	3.31E-07	no change
ENSMUSG00000025613	Cct8	-0.50534192	2.25E-07	no change
ENSMUSG00000001305	Rrp15	-0.627932248	5.27E-07	no change
ENSMUSG00000005410	Mcm5	-0.715976529	5.32E-07	no change
ENSMUSG00000038910	Plcl2	1.262256681	1.35E-06	no change
ENSMUSG00000022893	Adamts1	-1.055691385	2.28E-06	no change
ENSMUSG00000064373	Sepp1	1.286570881	3.01E-06	no change
ENSMUSG00000005413	Hmox1	-0.760855197	5.85E-06	no change
ENSMUSG00000064061	Dzip3	0.689109328	6.19E-06	no change
ENSMUSG00000049672	Zfp161	0.831844504	2.31E-05	no change
ENSMUSG00000083169	Gm6580	-0.992553755	5.94E-05	no change
ENSMUSG00000027692	Tnik	-1.05920674	7.67E-05	no change
ENSMUSG00000020547	Bzw2	-0.452773557	4.59E-05	no change
ENSMUSG00000019769	Syne1	0.806200347	0.000165789	no change
ENSMUSG00000026107	Obfc2a	-0.686434866	0.000249739	no change
ENSMUSG00000058325	Dock1	0.513897871	0.000282341	no change
ENSMUSG00000024431	Nr3c1	0.594736278	0.000834911	no change
ENSMUSG00000034472	Rasd2	-0.976149857	0.003112244	no change
ENSMUSG00000033352	Map2k4	0.32092198	0.001191664	no change
ENSMUSG00000030657	Xylt1	-1.02409107	0.003290214	no change
ENSMUSG00000054863	Fam19a5	-0.540234062	0.003520108	no change
ENSMUSG00000005124	Wisp1	-1.286136385	0.007305304	no change
ENSMUSG00000022335	Zfat	-0.514587106	0.004751429	no change
ENSMUSG00000032452	Clstn2	1.433461863	0.01271206	no change
ENSMUSG00000013846	St3gal1	0.865521376	0.012340628	no change
ENSMUSG00000022111	Uchl3	-0.399910181	0.00799824	no change
ENSMUSG00000020638	Cmpk2	1.351462304	0.024559191	no change
ENSMUSG00000039210	Gpatch2	0.346689688	0.00752337	no change
ENSMUSG00000033083	Tbc1d4	-0.503189347	0.017748527	no change

ENSMUSG00000022021	Diap3	0.261427737	0.011451482	no change
ENSMUSG00000029629	Phf14	0.220683146	0.00968961	no change
ENSMUSG00000080776	Gm12174	0.28499607	0.00962685	no change
ENSMUSG00000053199	Arhgap20	1.137927357	0.04075692	no change
ENSMUSG00000030209	Grin2b	-1.53656035	0.051218156	no change
ENSMUSG00000052299	Ltn1	-0.311842264	0.011480296	no change
ENSMUSG00000020542	Myocd	-1.05834225	0.056605617	no change
ENSMUSG00000027160	Ccdc34	0.482503713	0.020393391	no change
ENSMUSG00000029632	Ndufa4	0.251518793	0.016285105	no change
ENSMUSG00000036192	Rorb	1.186366656	0.086295865	no change
ENSMUSG00000036334	Igsf10	0.438989169	0.022808098	no change
ENSMUSG00000049107	Ntf3	1.167043888	0.104418649	no change
ENSMUSG00000072244	Trim6	-0.236733915	0.029705154	no change
ENSMUSG00000025612	Bach1	0.18927053	0.027486219	no change
	A430105J06R			
ENSMUSG00000090488	ik	0.786744981	0.115505283	no change
ENSMUSG00000021719	Rgs7bp	-0.635326311	0.129160137	no change
ENSMUSG00000020672	Sntg2	-0.899963831	0.144297375	no change
ENSMUSG00000063632	Sox11	0.335025677	0.031283332	no change
ENSMUSG00000073805	Fam196a	0.721026368	0.137312091	no change
	C030034I22Ri			
ENSMUSG00000073374	k	0.649989713	0.202986418	no change
ENSMUSG00000034518	Hmgxb4	0.159868927	0.043778598	no change
ENSMUSG00000026610	Esrrg	-0.903884629	0.235332437	no change
ENSMUSG00000042870	Tom1	0.684757282	0.245070313	no change
ENSMUSG00000057604	Lmcd1	-0.61991049	0.345641812	no change
ENSMUSG00000081277	Gm15285	0.566452268	0.269412711	no change
ENSMUSG00000032036	Kirrel3	-0.504393965	0.380504565	no change
ENSMUSG00000044442	N6amt1	-0.262071625	0.187610518	no change
ENSMUSG00000018347	Zkscan6	0.194567187	0.158152161	no change
ENSMUSG00000064315	Rpl21-ps10	0.309876165	0.565432064	no change
ENSMUSG00000084169	Gm12240	0.321026462	0.613684955	no change
ENSMUSG00000055435	Maf	-0.282839498	0.602350478	no change
ENSMUSG00000049336	Odz2	0.258185598	0.593523545	no change
ENSMUSG00000024044	Epb4.1i3	-0.133234211	0.121829462	no change
ENSMUSG00000028180	Zranb2	0.124337791	0.103611521	no change
ENSMUSG00000033060	Lmo7	-0.243463654	0.262340842	no change
ENSMUSG00000020577	Tspan13	0.194191669	0.153696306	no change
	C330027C09			
ENSMUSG00000033031	Rik	0.147962336	0.113587099	no change
ENSMUSG00000027695	Pld1	-0.005885565	0.991480201	no change
ENSMUSG00000083372	Gm11235	-0.263015615	0.61414884	no change
ENSMUSG00000059301	Gm5434	-0.191456267	0.682174494	no change
ENSMUSG00000039126	Prune2	0.261850631	0.209426315	no change
ENSMUSG00000090607	Gm17052	-0.169373926	0.518170478	no change
ENSMUSG00000044864	Ankrd50	0.168027556	0.148412884	no change
ENSMUSG00000081151	Gm11448	0.100469708	0.781856459	no change
ENSMUSG00000036452	Arhgap26	0.198925145	0.424006179	no change
ENSMUSG00000048482	Bdnf	-0.051588102	0.913564804	no change
ENSMUSG00000044645	Gm7334	-0.165556808	0.416170838	no change
ENSMUSG00000039224	D1Pas1	0.159097787	0.635932371	no change
ENSMUSG00000027162	Lin7c	0.106918878	0.187500575	no change
ENSMUSG00000039384	Dusp10	-0.045130212	0.850477409	no change
ENSMUSG00000041079	Rwdd2b	0.086308654	0.744101904	no change
ENSMUSG00000078908	Mon1b	-0.074205634	0.755882771	no change
ENSMUSG00000075486	Commd6	0.083065529	0.703561229	no change
ENSMUSG0000005125	Ndrg1	-0.152567564	0.340950087	no change
ENSMUSG00000020642	Rnf144a	-0.082367065	0.526179254	no change

ENSMUSG00000090946	2010109K11Rik	-0.027259893	0.887812123	no change
ENSMUSG00000024712	Rfk	-0.054026346	0.605105819	no change
ENSMUSG00000036188	Ankmy2	-0.008915519	0.947999739	no change
ENSMUSG00000044285	Gm1821	0.036520121	0.858291556	no change
ENSMUSG00000025616	Usp16	0.005020207	0.966080444	no change

**Table S10. Fold Change of D6 RA in RA-specific domain loss**

ENSEMBL	SYMBOL	Log <sub>2</sub> FC	adj.P.Val	Regulation
ENSMUSG00000024501	Dpysl3	4.601551012	1.56E-16	up
ENSMUSG00000022892	App	2.428596558	1.24E-15	up
ENSMUSG00000042834	D0H4S114	3.463869816	7.39E-15	up
ENSMUSG00000029838	Ptn	4.545941986	2.48E-14	up
ENSMUSG00000020601	Trib2	2.151937429	4.49E-14	up
ENSMUSG00000017491	Rarb	5.460364079	3.26E-14	up
ENSMUSG00000050334	C130071C03Rik	7.209586634	4.82E-14	up
ENSMUSG00000022629	Kif21a	1.917190588	9.17E-14	up
ENSMUSG00000022454	Nell2	3.508660557	1.61E-13	up
ENSMUSG00000029534	St7	2.900377333	1.92E-13	up
ENSMUSG00000040943	Tet2	2.863924491	3.16E-13	up
ENSMUSG00000006586	Runx1t1	1.795087323	5.64E-13	up
ENSMUSG00000036478	Btg1	2.474637996	5.90E-13	up
ENSMUSG00000022708	Zbtb20	4.185502496	7.50E-13	up
ENSMUSG00000053477	Tcf4	2.2815475	7.90E-13	up
ENSMUSG00000024502	Jakmip2	1.609276969	1.86E-12	up
ENSMUSG00000049001	A930038C07Rik	6.558767583	1.27E-12	up
ENSMUSG00000052062	Pard3b	3.29818005	5.40E-11	up
ENSMUSG00000090386	2810055G20Rik	8.066865842	1.19E-11	up
ENSMUSG00000015243	Abca1	2.555644353	2.76E-10	up
ENSMUSG00000020948	Klhl28	1.716761342	6.33E-10	up
ENSMUSG00000025810	Nrp1	3.596030149	1.12E-09	up
ENSMUSG00000047261	Gap43	1.609371994	8.81E-10	up
ENSMUSG00000063600	Egfem1	3.304808613	1.41E-09	up
ENSMUSG00000042514	Klhl14	5.736329508	1.11E-09	up
ENSMUSG00000039954	Stk32a	2.044532509	1.46E-09	up
ENSMUSG00000052450	2810055G20Rik	5.962007225	1.14E-09	up
ENSMUSG00000038349	Plcl1	6.46280701	1.39E-09	up
ENSMUSG00000039782	Cpeb2	2.953521168	4.39E-09	up
ENSMUSG00000079157	Fam155a	3.42267792	5.05E-09	up
ENSMUSG00000064325	Hhip	2.920263066	1.44E-08	up
ENSMUSG00000087060	2810442I21Rik	1.735950646	4.38E-08	up
ENSMUSG00000038128	Camk4	2.436992039	8.68E-08	up
ENSMUSG00000043518	Rai2	3.98736903	9.18E-07	up
ENSMUSG00000066842	Hmcn1	1.788801775	2.72E-06	up
ENSMUSG00000052560	Cpne8	2.93375638	4.85E-06	up
ENSMUSG00000087565	Gm14662	3.382486897	5.15E-05	up
ENSMUSG00000055370	Gm9968	2.487048998	8.72E-05	up
ENSMUSG00000053025	Sv2b	1.513859964	0.002203861	up
ENSMUSG00000020116	Pno1	-1.738496877	3.04E-14	down
ENSMUSG00000022367	Has2	-3.587289188	1.39E-13	down
ENSMUSG00000031139	Mcf2	-4.943065812	1.22E-12	down
ENSMUSG00000090744	Gm6871	-2.703845374	2.12E-12	down
ENSMUSG00000027955	Fam198b	-3.307834992	7.52E-12	down
ENSMUSG00000040569	Slc26a7	-4.184057877	6.98E-06	down
ENSMUSG00000054951	9130008F23Rik	-3.493903875	4.60E-05	down
ENSMUSG00000022865	Cxadr	1.455442928	1.69E-12	no change
ENSMUSG00000017485	Top2b	1.152516896	3.86E-12	no change

ENSMUSG00000035762	Tmem161b	1.199442342	7.43E-10	no change
ENSMUSG00000028030	Tbck	1.267387939	1.54E-09	no change
ENSMUSG00000062949	Atp11c	1.25242335	3.77E-09	no change
ENSMUSG00000029910	Mad2l1	-0.756165586	8.55E-09	no change
ENSMUSG00000040550	Otud6b	-0.757185049	1.04E-08	no change
ENSMUSG00000047534	Mis18bp1	-0.723599339	1.80E-08	no change
ENSMUSG00000078970	Wdr92	-0.853860778	4.08E-08	no change
ENSMUSG00000043424	Gm9781	-0.810149475	8.50E-08	no change
ENSMUSG00000028018	Gstcd	-0.76128593	1.05E-07	no change
ENSMUSG00000048490	Nrip1	1.054058882	2.19E-07	no change
ENSMUSG00000035597	Prpf39	0.498109402	3.34E-07	no change
ENSMUSG00000075470	Alg10b	0.712145838	8.47E-07	no change
ENSMUSG00000022867	Usp25	0.536676714	1.34E-06	no change
ENSMUSG00000020949	Fkbp3	-0.650616646	1.65E-06	no change
ENSMUSG00000044966	Fbxo48	1.289029634	4.43E-06	no change
ENSMUSG00000044629	Cnrip1	0.683416954	4.45E-06	no change
ENSMUSG00000021548	Ccnh	-0.481815429	4.01E-06	no change
ENSMUSG00000028013	Ppa2	-0.533377837	4.99E-06	no change
ENSMUSG00000053819	Camk2d	0.497148268	6.38E-06	no change
ENSMUSG0000000581	C1d	-0.692328883	5.44E-06	no change
ENSMUSG00000021549	Rasa1	0.42900838	5.57E-06	no change
ENSMUSG00000029552	Tes	-0.604358357	1.72E-05	no change
ENSMUSG00000026771	Spopl	0.474288213	1.79E-05	no change
ENSMUSG00000028029	Aimp1	-0.501408408	1.91E-05	no change
ENSMUSG00000027684	Mecom	0.763549868	3.70E-05	no change
ENSMUSG00000047227	Gm527	1.365197327	0.000183428	no change
ENSMUSG00000074166	AW146154	-0.607138128	0.000110586	no change
ENSMUSG00000028221	Tmem55a	-0.424279065	7.25E-05	no change
ENSMUSG00000023921	Mut	-0.416518077	0.000238297	no change
ENSMUSG00000040998	Nppt	1.026515427	0.000613398	no change
ENSMUSG00000079575	Rbpsuh-rs3	0.401131816	0.00033398	no change
ENSMUSG00000006010	BC003331	0.364290662	0.000315885	no change
ENSMUSG00000059493	Nhs	-0.523790958	0.00055697	no change
ENSMUSG00000021785	Ngly1	0.606362652	0.000954972	no change
ENSMUSG00000005583	Mef2c	0.863880629	0.001408304	no change
ENSMUSG00000022314	Rad21	0.197902824	0.000765758	no change
ENSMUSG00000065855	U6	1.266763493	0.006021434	no change
ENSMUSG00000006005	Tpr	-0.263669006	0.00114978	no change
ENSMUSG00000078974	Sec61g	0.649404623	0.004000365	no change
ENSMUSG00000024642	Tle4	-0.285255728	0.001885784	no change
ENSMUSG00000022863	Btg3	-0.68696427	0.008293081	no change
ENSMUSG00000050299	Gm9843	-0.352071201	0.003000104	no change
ENSMUSG00000028016	Ints12	0.254545033	0.008503596	no change
ENSMUSG00000015247	Nipsnap3b	0.26148117	0.011577602	no change
ENSMUSG00000026986	Hnmt	-0.727801857	0.051815201	no change
ENSMUSG00000042742	B630005N14Rik	-0.259294623	0.012502554	no change
ENSMUSG00000048188	Gm8181	0.329464093	0.027083601	no change
ENSMUSG00000020120	Plek	0.66827749	0.045746806	no change
ENSMUSG00000023919	Cenpq	-0.260584961	0.016546437	no change
ENSMUSG00000024378	Stard4	0.396705052	0.02019588	no change
ENSMUSG00000022338	Eny2	0.208977417	0.019179879	no change
ENSMUSG00000020122	Egfr	0.380806856	0.053544601	no change
ENSMUSG00000071273	Gm5145	-0.400968191	0.131641429	no change
ENSMUSG00000045179	Sox3	0.244942419	0.060260767	no change
ENSMUSG00000029090	Gpr125	0.191347427	0.040996724	no change
ENSMUSG00000022864	D16Ert472e	-0.20928436	0.075880144	no change
ENSMUSG00000022313	Utp23	-0.196319334	0.072235008	no change
ENSMUSG00000028184	Lphn2	0.335597914	0.043871445	no change

ENSMUSG00000035614	Fam179b	-0.144009664	0.058401491	no change
ENSMUSG00000067870	Gm8759	-0.195621471	0.049251921	no change
ENSMUSG00000007655	Cav1	0.042627227	0.934143023	no change
ENSMUSG00000006014	Prg4	0.002496603	0.994756545	no change
ENSMUSG00000019966	Kitl	0.244800828	0.426476887	no change
ENSMUSG00000029913	Prdm5	0.138423733	0.5303766	no change
ENSMUSG00000009376	Met	-0.166077712	0.247107578	no change
ENSMUSG00000040282	BC052040	0.174414589	0.251551199	no change
ENSMUSG00000046934	Csl	0.13682832	0.420479236	no change
ENSMUSG00000021786	Oxsm	0.078916244	0.724623387	no change
ENSMUSG00000015733	Capza2	-0.079930343	0.15961489	no change
ENSMUSG00000022312	Eif3h	0.106268134	0.177886381	no change
ENSMUSG00000033953	Ppp3r1	0.082786442	0.219978808	no change
ENSMUSG00000029569	Tmem168	-0.084724595	0.310827601	no change
ENSMUSG00000055884	Fancm	0.08785255	0.365920781	no change
ENSMUSG00000057147	Atpbd4	-0.06199549	0.475320744	no change
ENSMUSG00000042680	Fam59a	-0.002651282	0.98454554	no change

**Table S11. Fold Change of D6 DMSO in DMSO-specific domain loss**

ENSEMBL	SYMBOL	Log <sub>2</sub> FC	adj.P.Val	Regulation
ENSMUSG00000064373	Sepp1	2.452798495	3.92E-11	up
ENSMUSG00000042659	Arrdc4	2.089323409	4.22E-11	up
ENSMUSG00000013846	St3gal1	3.30979863	1.47E-10	up
ENSMUSG00000055737	Ghr	1.819269007	3.47E-10	up
ENSMUSG00000038910	Plcl2	1.88188842	3.90E-10	up
ENSMUSG00000074968	Ano3	3.68549334	1.13E-09	up
ENSMUSG00000029765	Plxna4	2.851522982	1.37E-08	up
ENSMUSG00000020542	Myocd	2.878513586	1.79E-08	up
ENSMUSG00000027695	Pld1	2.456817915	9.41E-07	up
ENSMUSG00000005124	Wisp1	1.678574515	1.24E-06	up
ENSMUSG00000055435	Maf	2.012059212	6.33E-06	up
ENSMUSG00000021536	Adcy2	1.976047147	6.81E-06	up
ENSMUSG00000048482	Bdnf	1.560696893	1.93E-05	up
ENSMUSG00000049336	Odz2	1.610138246	5.84E-05	up
ENSMUSG00000056752	Dnahc9	2.060997301	0.000852923	up
ENSMUSG00000036192	Rorb	1.577842543	0.00573688	up
ENSMUSG00000045573	Penk	-4.145521923	2.94E-11	down
ENSMUSG0000005125	Ndrg1	-2.240844101	7.18E-11	down
ENSMUSG00000091002	Tcerg1l	-3.218315964	5.42E-10	down
ENSMUSG00000064315	Rpl21-ps10	-1.831454521	0.001253066	down
ENSMUSG00000030209	Grin2b	-1.978706569	0.00205888	down
ENSMUSG00000020524	Gria1	-1.919695876	0.002711199	down
ENSMUSG00000025613	Cct8	-1.191802414	5.98E-13	no change
ENSMUSG00000050199	Lgr4	-1.19957373	4.13E-11	no change
ENSMUSG00000054143	Hmox1	-1.358394265	1.51E-10	no change
ENSMUSG00000022019	Tdrd3	1.244680248	1.76E-10	no change
ENSMUSG00000005410	Mcm5	-1.161962267	1.35E-10	no change
ENSMUSG00000022893	Adamts1	1.268193287	2.13E-10	no change
ENSMUSG00000064061	Dzip3	1.273444568	2.31E-10	no change
ENSMUSG00000072244	Trim6	-1.00288166	1.65E-09	no change
ENSMUSG00000054863	Fam19a5	-1.497316215	2.43E-09	no change
ENSMUSG00000019769	Syne1	1.347381193	1.56E-08	no change
ENSMUSG00000083169	Gm6580	-1.320031413	1.91E-08	no change
ENSMUSG00000022021	Diap3	0.72030648	3.40E-08	no change
ENSMUSG00000029632	Ndufa4	-0.806817242	5.30E-08	no change
ENSMUSG00000022111	Uchl3	-0.897389662	1.32E-07	no change
ENSMUSG00000027692	Tnik	-1.171654381	2.13E-07	no change

ENSMUSG00000024431	Nr3c1	0.94637898	2.44E-07	no change
ENSMUSG00000001305	Rrp15	-0.533373758	2.25E-07	no change
ENSMUSG00000038843	Gcnt1	-0.816423108	7.95E-07	no change
ENSMUSG00000020547	Bzw2	-0.559293753	6.60E-07	no change
ENSMUSG00000034472	Rasd2	-1.492682509	1.68E-06	no change
ENSMUSG00000043061	Tmem18	0.672975755	1.33E-06	no change
ENSMUSG00000053930	Shisa6	-1.389091426	7.40E-06	no change
ENSMUSG00000024712	Rfk	-0.480853152	1.01E-05	no change
ENSMUSG00000039210	Gpatch2	0.561015226	1.31E-05	no change
ENSMUSG00000036188	Ankmy2	-0.549376278	1.59E-05	no change
ENSMUSG00000033060	Lmo7	-0.847077515	4.18E-05	no change
ENSMUSG00000028180	Zranb2	-0.319743184	9.48E-05	no change
ENSMUSG00000021719	Rgs7bp	-1.151088639	0.001434569	no change
ENSMUSG00000073805	Fam196a	1.3059528	0.001309024	no change
ENSMUSG00000049672	Zfp161	0.474837675	0.000808335	no change
ENSMUSG00000036452	Arhgap26	0.624407786	0.001443615	no change
ENSMUSG00000090488	A430105J06Rik	1.235293339	0.002724452	no change
ENSMUSG00000090946	2010109K11Rik	-0.478310173	0.001387453	no change
ENSMUSG00000026610	Esrrg	1.432075236	0.003383317	no change
ENSMUSG00000025612	Bach1	0.255259105	0.001257095	no change
ENSMUSG00000044864	Ankrd50	0.34995964	0.00139741	no change
ENSMUSG00000073374	C030034I22Rik	1.106425319	0.006509441	no change
ENSMUSG00000027160	Ccdc34	0.556041017	0.002046117	no change
ENSMUSG00000042870	Tom1	1.209971109	0.009713808	no change
ENSMUSG00000020672	Sntg2	-1.213586124	0.011835622	no change
ENSMUSG00000029629	Phf14	0.224354117	0.002831849	no change
ENSMUSG00000033352	Map2k4	0.243346608	0.003246921	no change
ENSMUSG00000033031	C330027C09Rik	-0.261360525	0.003251273	no change
ENSMUSG00000041079	Rwdd2b	-0.539082237	0.008931015	no change
ENSMUSG00000020642	Rnf144a	0.283908773	0.005324814	no change
ENSMUSG00000058325	Dock1	0.305437966	0.005737344	no change
ENSMUSG00000039224	D1Pas1	0.595540378	0.013298913	no change
ENSMUSG00000081277	Gm15285	-1.03425114	0.028653336	no change
ENSMUSG00000052299	Ltn1	-0.288521832	0.006526336	no change
ENSMUSG00000084169	Gm12240	1.000959751	0.028709763	no change
ENSMUSG00000049107	Ntf3	1.180873079	0.043712006	no change
ENSMUSG00000063632	Sox11	0.349484255	0.009743251	no change
ENSMUSG00000090607	Gm17052	-0.396129506	0.036607106	no change
ENSMUSG00000020577	Tspan13	-0.254924839	0.025832937	no change
ENSMUSG00000081151	Gm11448	0.384780575	0.115692307	no change
ENSMUSG00000033083	Tbc1d4	0.249508757	0.064711548	no change
ENSMUSG00000057604	Lmcd1	-0.53452615	0.290774819	no change
ENSMUSG00000039384	Dusp10	0.259857296	0.094396112	no change
ENSMUSG00000036334	Igfsf10	0.297229954	0.055963007	no change
ENSMUSG00000018347	Zkscan6	0.175944712	0.091568067	no change
ENSMUSG00000075486	Commd6	-0.241418261	0.12082896	no change
ENSMUSG00000020638	Cmpk2	-0.346294791	0.518283027	no change
ENSMUSG00000027162	Lin7c	-0.136188046	0.057345005	no change
ENSMUSG00000044285	Gm1821	-0.273887133	0.075715985	no change
ENSMUSG00000032036	Kirrel3	-0.324372313	0.42746033	no change
ENSMUSG00000053199	Arhgap20	0.303914334	0.503575381	no change
ENSMUSG00000024044	Epb4.1i3	0.116544812	0.099237812	no change
ENSMUSG00000032452	Clstn2	0.151750844	0.758369844	no change
ENSMUSG00000078908	Mon1b	0.183051662	0.241374069	no change
ENSMUSG00000030657	Xylt1	-0.201798271	0.290151712	no change
ENSMUSG00000083372	Gm11235	-0.182721844	0.609208714	no change
ENSMUSG00000044645	Gm7334	0.154076782	0.26760758	no change
ENSMUSG00000059301	Gm5434	-0.039950961	0.901837397	no change

ENSMUSG00000026107	Obfc2a	-0.131179983	0.217645359	no change
ENSMUSG00000039126	Prune2	-0.175106081	0.286378167	no change
ENSMUSG00000044442	N6amt1	-0.091432776	0.503249152	no change
ENSMUSG00000057143	Trim12c	-0.106339701	0.438042723	no change
ENSMUSG00000025616	Usp16	0.083892411	0.32085697	no change
ENSMUSG00000022335	Zfat	-0.048987344	0.675030863	no change
ENSMUSG00000034518	Hmgxb4	0.018526754	0.782936908	no change
ENSMUSG00000080776	Gm12174	-0.022768683	0.804116034	no change



**Movie 1.** DMSO treatment differentiates P19 cells into beating cardiomyocytes.